EUROPEAN COMMISSION

Community research

Long-term Performance of Engineered Barrier Systems

PEBS

Long-term Performance of Engineered Barrier Systems PEBS

Laboratory studies on stress-strain behavior

(DELIVERABLE-N°: D2.2-12)

Contract (grant agreement) number: FP7 249681

Author(s):

A. Dueck Clay Technology AB

Reporting period: 01/03/10 – 28/02/14

Date of issue of this report: 20/02/14

Start date of project: 01/03/10 Duration : 48 Months

Project co-funded by the European Commission under the Seventh Euratom Framework Programme for Nuclear Research &Training Activities (2007-2011)		
Dissemination Level		
PU	Public	**PU**
RE	Restricted to a group specified by the partners of the [acronym] project	
CO	Confidential, only for partners of the [acronym] project	

EURATOM

Table of Contents

1 Introduction

1.1 Background

This study on stress-strain behaviour has been done within the EU-project PEBS and the Task *Experimentation on key THM processes and parameters* (PEBS, 2010) to better understand the mechanical properties of buffer material exposed to increased temperature during and after water saturation. Thermo-mechanically induced brittleness has previously been observed in buffer material (Karnland et al. 2009, Åkesson et al. 2012, Dueck et al. 2011) and further studies regarding the origin of brittleness has been of importance to further understand the behaviour. The mechanical properties of bentonite has therefore been studied by laboratory tests as unconfined compression tests and swelling pressure tests.

1.2 Objective

The objective has been to further investigate the influence of temperature and factors coupled to increased temperature. Specific topics have been effects of heating at different degrees of saturation and effects of different an-ions. In addition to unconfined compression tests, swelling pressure and hydraulic conductivity tests on specimens exposed to increased temperature have also been of interest.

1.3 Unconfined compression tests in the LOT project

Buffer material exposed to repository and accelerating conditions involving increased temperature were investigated in the project LOT at Äspö HRL, Sweden (Karnland et al. 2009). Stress-strain behaviour in different positions in the LOT parcel and in reference material was determined by unconfined compression tests.

An example of test results from unconfined compression tests in the LOT project (Karnland et al., 2009) is shown in Figure 1-1. The Figure shows results from the parcel material as deviator stress versus strain and the colours refer to the temperature coupled to the positions of the specimens in the LOT parcel. From the warmest to the coldest the colours red, orange, yellow and green represent the average temperatures 125˚C, 115˚C, 100˚C and 90˚C, respectively. The density of each specimen is shown to the right in the diagram. The black lines refer to results from reference material.

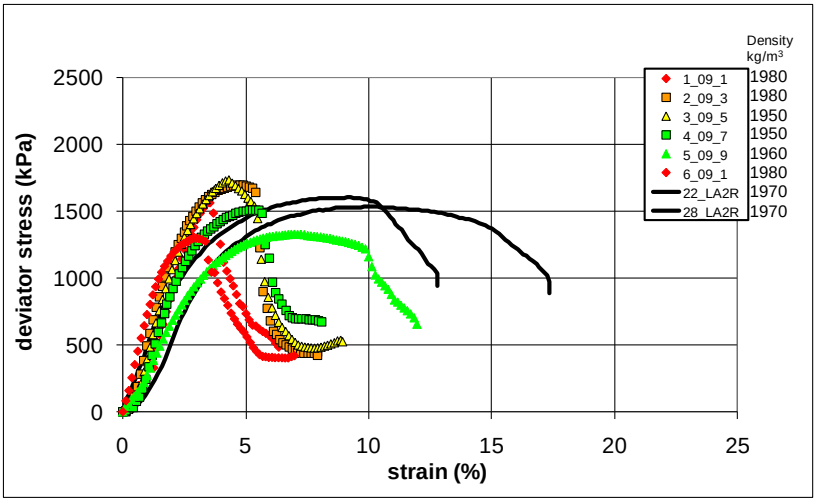

Figure 1-1. *Deviator stress versus strain resulting from unconfined compression tests on material from the LOT project (Karnland et al., 2009).*

The most important conclusions from the LOT project concerning the results from the unconfined compression tests were that for the material from the warm section significantly reduced strain at failure was measured and that a qualitatively different course of shearing involving a more pronounced failure was noticed. Test series with material not exposed to field conditions but heated in a laboratory oven showed a correlation between lower strains at failure and increasing temperature despite the short exposure time in the laboratory oven.

2 Analyses and test techniques

2.1 General

The stress-strain behaviour was determined by unconfined compression tests. This test type was used in all test series. In the series where the specimens were exposed to heating the stress-strain behaviour was complemented by determination of swelling pressure and hydraulic conductivity. For some specimens the relative humidity was measured above the dismantled specimens and in these cases the corresponding suction was calculated and used as a measure of the swelling pressure.

2.2 Water content, density and relative humidity determination

The base variables water content w (%), void ratio e, and degree of saturation S_r (%) were determined according to Equations 2-1 to 2-3.

$$w = 100 \cdot \frac{m_{tot} - m_s}{m_s} \tag{2-1}$$

$$e = \frac{\rho_s}{\rho}(1 + w/100) - 1 \tag{2-2}$$

$$S_r = \frac{\rho_s \cdot w}{\rho_w \cdot e} \tag{2-3}$$

where

m_{tot} = total mass of the specimen (kg)
m_s = dry mass of the specimen (kg)
ρ_s = particle density (kg/m^3)
ρ_w = density of water (kg/m^3)
ρ = bulk density of the specimen (kg/m^3)

The dry mass of the specimen was obtained from drying the wet specimen at 105˚C for 24h. The bulk density was calculated from the total mass of the specimen and the volume determined by weighing the specimen above and submerged into paraffin oil.

The relative humidity *RH* (%) was measured by capacitive sensors. The sensors were calibrated above saturated salt solutions being attached to a calibration device. The same device was also used for the measurement of *RH* of buffer samples with the salt solution exchanged for the actual sample.

The relative humidity is defined according to Equation 2-4. From the relative humidity the corresponding suction ψ (kPa) can be determined according to the thermodynamic equation, Equation 2-5, given by e.g. Fredlund and Rahardjo (1993).

$$RH = 100 \cdot \frac{p}{p_s} \qquad (2\text{-}4)$$

where

p = partial pressure of pore-water vapour (kPa)
p_s = saturation pressure of water vapour over a flat surface of pure water at the same temperature (kPa)

$$\psi = -\frac{R \cdot T}{v_{w0} \cdot \omega_v} \ln\left(\frac{p}{p_s}\right) \qquad (2\text{-}5)$$

where

T = absolute temperature (K)
R = universal gas constant (8.31432 J/(mol K))
v_{w0} = specific volume of water ($1/\rho_w$ m^3/kg)
ω_v = molecular mass of water vapour (18 kg/kmol)

RH measurements or calculated suction values can be used as a measure of the swelling pressure. Correspondence between water retention properties in terms of chemical potential, *RH* or suction and swelling pressure under certain conditions has previously been shown by e.g. Kahr et al. (1990) and Karnland et al. (2005) and Dueck and Börgesson (2007).

2.3 Heating of specimens

Some specimens were heated during the preparation. These specimens were, still inside the saturation device, exposed to an increased temperature between T = 90˚C - 150˚C during 24h. The heating was made either after or before full saturation. In case of heating after saturation a water pressure of 600 kPa was applied to the specimens during the heating. After the heating the water pressure was lowered and water with atmospheric pressure was again supplied to the specimens.

The specimens heated before full saturation were water supplied during a couple of minutes after evacuating air from filter and tubes and subsequently the specimens were placed into the oven, sealed but without controlled pressure. After the heating water with atmospheric pressure was supplied to the specimens.

The heated specimens were kept in the saturation device at room temperature some additional time to homogenise before the dismantling. After dismantling the specimens were used for the unconfined compression test or the combined swelling pressure – hydraulic conductivity tests described in section 2.4 and section 2.5, respectively. In addition, some extra specimens were used for measurements of relative humidity and interpreted according to section 2.2.

2.4 Unconfined compression test

The unconfined compression test has been used in several studies where the mechanical or physical properties of bentonite were of interest (Börgesson et al., 2004, Dueck et al., 2010). The method has also been used to evaluate the relative physical changes between specimens treated differently (Karnland et al., 2009, Dueck et al., 2011, Åkesson et al., 2012).

The unconfined compression test is an experimentally simple method where a specimen is compressed axially with a constant rate of deformation and no radial confinement or external radial stress. The cylindrical specimen is compressed to shear failure. The dimensions of the specimen are often a height which is double the size of the diameter to allow for the shear failure to develop without boundary effects from the end surfaces. However, in the present study the height of the specimens has been equal to the diameter and to minimize the end effects of the short specimens the end surfaces were lubricated.

2.4.1 Equipment

The specimens were saturated in a special designed saturation device before the shear test. The shearing was made by a mechanical press and a set up shown in Figure 2-1. During the test the deformation and the applied force were measured by means of a standard load cell and a deformation transducer. All transducers were calibrated prior to the shearing of one series and checked afterwards.

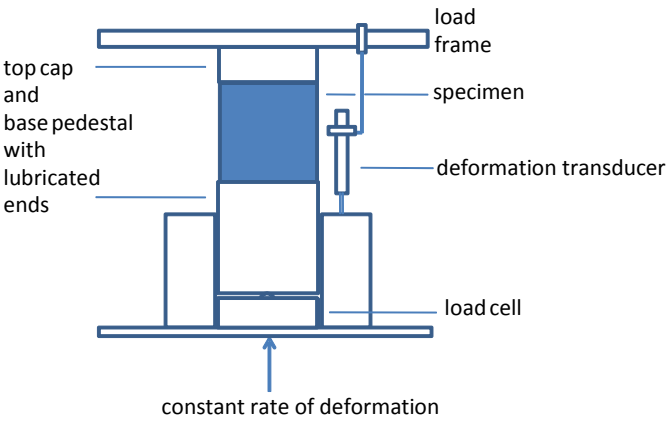

Figure 2-1. Set-up for the unconfined compression test.

2.4.2 Preparation of specimen

The specimens were prepared in a compaction device from powder to cylindrical specimens, 20 mm in diameter and 20 mm in height. The specimens were saturated with de-ionized water applied after evacuating the steel filters and tubes in the saturation device. During the saturation a minor water pressure of approximately 2 kPa was applied. After saturation during more than a two-week period the specimens were removed from the saturation device at least 12h before the shearing.

Some specimens were heated during the preparation and still inside the saturation device these specimens were treated according to section 2.3.

2.4.3 Test procedure

At shearing the specimens were placed in the mechanical press and the compression started and continued at a constant deformation rate of 0.16 mm/min (or 0.003 mm/s). To minimize boundary effects from the top and bottom during shearing the specimen's ends were lubricated by use of vacuum grease. During shearing the specimens were surrounded by a protective plastic sheet to prevent or minimize evaporation. After failure the water content and density were determined according to section 2.2.

The specimens were considered as undrained during shearing and no volume change was taken into account. The deviator stress q (kPa) and the strain ε (%) were derived from Equations 2-6 and 2-7, respectively. The results were corrected for initial problems with the contact surface in that decreasing the strain with the intercept on the x-axis, strain-axis, of the tangent to the stress-strain curve taken at a stress of 500 kPa.

$$q = \frac{F}{A_0} \cdot \left(\frac{l_0 - \Delta l}{l_0}\right) \qquad (2\text{-}6)$$

$$\varepsilon = \frac{\Delta l}{l_0} \qquad (2\text{-}7)$$

where

F = applied vertical load (kN)
A_0 = original cross section area (m^2)
l_0 = original length (m)
Δl = change in length (m)

2.5 Swelling pressure and hydraulic conductivity tests

The hydraulic conductivity and swelling pressure were determined in a combined test in a swelling pressure device. The method has been commonly used for the determination of sealing properties (e.g. Karnland et al. 2009, Dueck et al., 2011, Åkesson et al. 2012). The determined parameters are related to the density of the sample and the chemical composition of the water and the buffer material (Karnland et al., 2006).

2.5.1 Test equipment

The hydraulic conductivity and swelling pressure were determined by use of the test equipment shown in Figure 2-2, made of acid proof stainless steel. The specimens were confined by a cylinder ring with a diameter of 35 mm and stainless steel filters at the top and bottom end surfaces. The test volume was sealed by o - rings placed between the bottom plate and the cylinder ring and between the piston and the cylinder ring. At test start the height of the test volume was fixed to approximately 10 mm.

The axial force from the samples was determined by a load cell placed between the piston and the upper lid. The displacement of the piston due to transducer deformation is 25 μm at maximum force, which consequently correspond to 0.25% of the sample height which was considered insignificant.

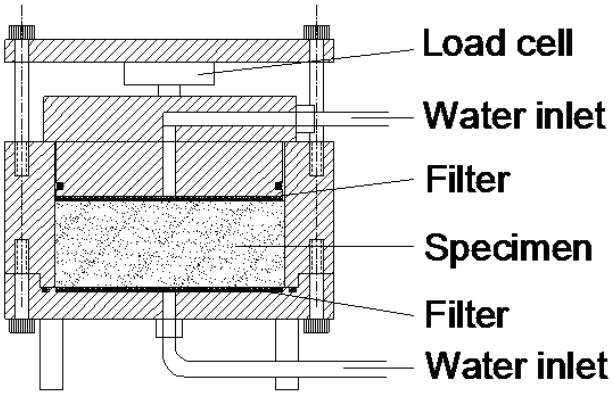

Figure 2-2. A schematic drawing of the swelling pressure device.

2.5.2 Preparation of specimen

The specimens were prepared in a compaction device from powder to cylindrical specimens, 35 mm in diameter and 10 mm in height. The specimens were placed in the swelling pressure device and saturated with de-ionized water applied after evacuating the steel filters and tubes. During the saturation during more than a two-week period a minor water pressure of approximately 2 kPa was applied. The swelling pressure was measured continuously.

Some specimens were heated during the preparation and those were placed as compacted specimens in a special saturation device where they were heated according to section 2.3. After the heating these specimens were dismantled from the saturation device and put into the swelling pressure device where de-ionised water was supplied again.

2.5.3 Test procedure

After saturation a water pressure gradient was applied over the specimens and the volume of the out-flowing water measured until stable rate was measured. The hydraulic conductivity was then calculated according to Darcy´s law. The gradient during the tests was between 3900 and 10600 m/m which corresponded to water pressure differences of 400 kPa and 1000 kPa, respectively over the specimens. The measurements of the outflow were made during several days in order to get stable values of the evaluated hydraulic conductivity. The water pressure was thereafter reduced to zero and the test was terminated when the recorded axial force was stable. The swelling pressure used for the interpretation was evaluated just before the termination and dismantling. The water content and density were determined for each specimen after the tests.

3 Materials and test series

3.1 General

Altogether 13 test series were carried out. The series were labelled series A to N. The letters are kept throughout the report. In this chapter each series is mentioned with the material and preparation used and also the purpose of each series. The special treatment necessary to meet the mentioned purpose of a series is described with the results from the actual series, in section 4.2 The influence is quantified by measurements of stresses and strains during the unconfined compression test and from some of the series also by results from the swelling pressure and hydraulic conductivity test. Both test types are described in general terms in Chapter 2.

3.2 Materials used

The bentonite mainly used in the test series was MX-80 which is a Wyoming bentonite product from American Colloid Co. In one series the purified WyNa was used and this material was ion exchanged from MX-80 to a Na bentonite with the accessory minerals removed, according to Karnland et al. (2006). Properties regarding mineralogy and sealing properties of MX-80 and WyNa were reported by Karnland et al. (2006). The particle densities used for these materials were ρ_s = 2780 kg/m^3 and ρ_s = 2750 kg/m^3, respectively and the water density used was ρ_w = 1000 kg/m^3.

The FEBEX bentonite was used in some test series and the FEBEX bentonite is a Mg-Ca bentonite extracted from Almería in Spain, exploited by the major Spanish bentonite producer, Minas de Gádor S.A. (now Süd-Chemie Espana). Properties of the FEBEX bentonite are presented e.g. by Villar (2002). The particle density and water density used for the FEBEX specimens were ρ_s = 2735 kg/m^3 (Svensson et al. 2011) and ρ_w = 1000 kg/m^3.

3.3 Test series

In Table 3-1 the material, test method, type of water, number of specimens, maximum temperature and the purpose of each series are shown.

Table 3-1. Purpose of each series and the material, preparation and test type used. Two test types were used; the unconfined compression tests (PUC) and the swelling pressure and hydraulic conductivity tests (PSP). In the column with the type of test used the number of specimens is included.

Series	Purpose of the test series	Material	Water other than de-ionized	Exposure to max T during 24h	Type of tests (PUC and PSP) and number of specimens
A	Influence of heat on purified Na bentonite	WyNa		150°C	PUC 4
B	Influence of grinding and separation of coarse fraction	MX-80		20°C	PUC 10
C	Influence of saturation with $CaCl_2$	MX-80	0.3M$CaCl_2$	20°C	PUC 6
D	Influence of introduced fractures	MX-80		20°C	PUC 10
E	Influence of circulation with Na_2SO_4	MX-80	1M Na_2SO_4	20°C	PUC 6
F	Influence of washing	MX-80		20°C	PUC 10
G	Influence of content of $CaSO_4$	MX-80 + $CaSO_4$		150°C	PUC 2
H	Influence of direction of compaction	MX-80		20°C	PUC 6
I	Check of variability	MX-80		20°C	PUC 10
K	Influence of heating before saturation	MX-80		20°C, 90°C, 120°C,150°C	PUC 15 PSP 8
L	Influence of heating after saturation	MX-80		20°C, 90°C, 120°C,150°C	PUC 9 PSP 8
M	Influence of heating before saturation	FEBEX		20°C, 90°C	PUC 8 PSP 6
N	Influence of heating after saturation	FEBEX		20°C, 90°C	PUC 8 PSP 6

4 Results

4.1 General

All tests carried out in this project are presented in separate sections below. Each section starts with a brief description of the objectives of the test series and details regarding deviations from the preparations and test procedures as they are presented in Chapter 2. In all test series, series A-N, the unconfined compression test was used to determine the stress-strain properties on specimens treated in different ways. In series K-N the swelling pressure and hydraulic conductivity test was also used.

In addition to the results presented below more details are given in Appendix A1 where diagrams with the stress-strain curves and the evolutions of swelling pressure are shown together with tables giving the test results from all tests. The swelling pressure given below was evaluated after removal of the water pressure used for the determination of hydraulic conductivity and just before the dismantling. In Appendix A1 the swelling pressure evaluated both before and after the introduction of water pressure are given. The hydraulic conductivity given below was evaluated without consideration of possible evaporation from the tubes during the measurements. In Appendix A1 the hydraulic conductivity is given both with and without an estimated evaporation.

4.2 Results from test series A-N

A. Influence of heat (150°C) on purified Na bentonite

Effects of heating on purified MX-80 (label: WyNa) was studied in this series. The series is the only one using purified MX-80 which is ion-exchanged MX-80, in this case ion-exchanged to be Na dominated, with accessory minerals removed. Some of the specimens were heated to 150°C during 24h. Two MX-80 reference specimens were also tested.

From the test results in *Figure 4-1* the purified WyNa specimens heated to 150°C shows increased maximum deviator stress q_{max} and decreased strain at q_{max} compared to the not heated WyNa specimens. The two specimens of MX-80 show no difference in deviator stress at failure although one specimen was heated to 150°C but regarding strain, decreased strain is seen after exposure to 150°C which was expected from other test series.

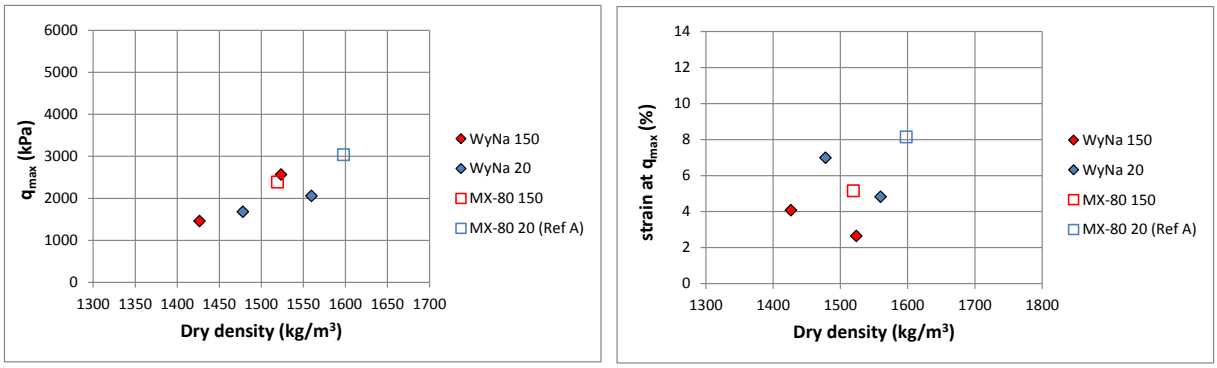

Figure 4-1. Maximum deviator stress q_{max} and corresponding strain ε as a function dry density from test series A.

B. Influence of grinding and separation of coarse fraction

Normally prepared specimens of MX-80 were in this series compared to specimens of ground MX-80 and specimens consisting of the ground fine fraction of MX-80 i.e. with the accessory minerals larger than 2 μm removed. The removal of the coarser fractions involved washing by de-ionized water, evaporation and grinding.

Interpreted from the test results in *Figure 4-2* grinding (yellow circles) seems not to have influenced the maximum deviator stress at failure q_{max} but a small increase in strain at failure is seen in the ground material. The fine fraction of MX-80 (red circles) show slightly increased q_{max} and decreased strain at q_{max} compared to the references (label: MX-80 Ref B) but the deviations may partly be explained by a decreased dry density after removal of the coarser material since the coarser part mainly consists of non-swelling accessory minerals.

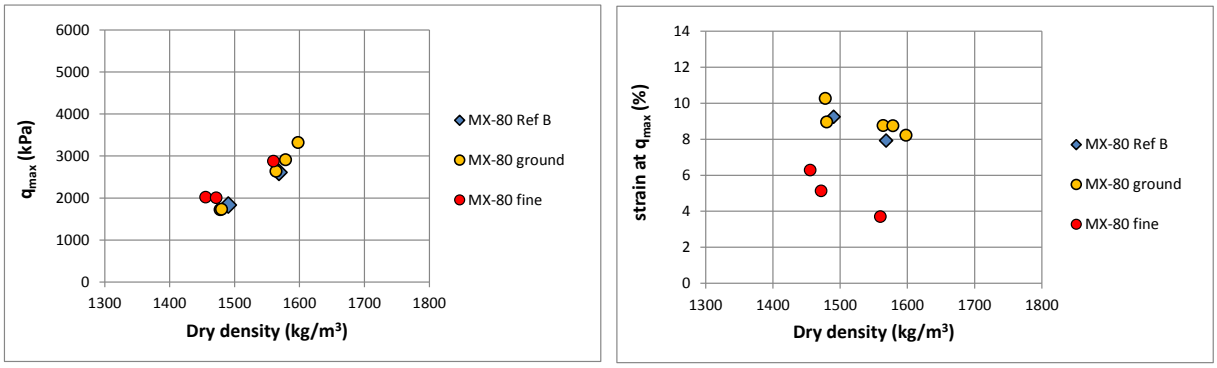

Figure 4-2. Maximum deviator stress q_{max} and corresponding strain ε as a function dry density from test series B.

C. Influence of saturation with $CaCl_2$

In this series specimens were saturated with de-ionized water or with a solution of 0.3M $CaCl_2$. The water and the solution were circulated at regular intervals above and under the specimens during 40 days. From the results in *Figure 4-3* no large difference is seen between the specimens being saturated with de-ionized water (label: MX-80 Ref C) and with 0.3M $CaCl_2$.

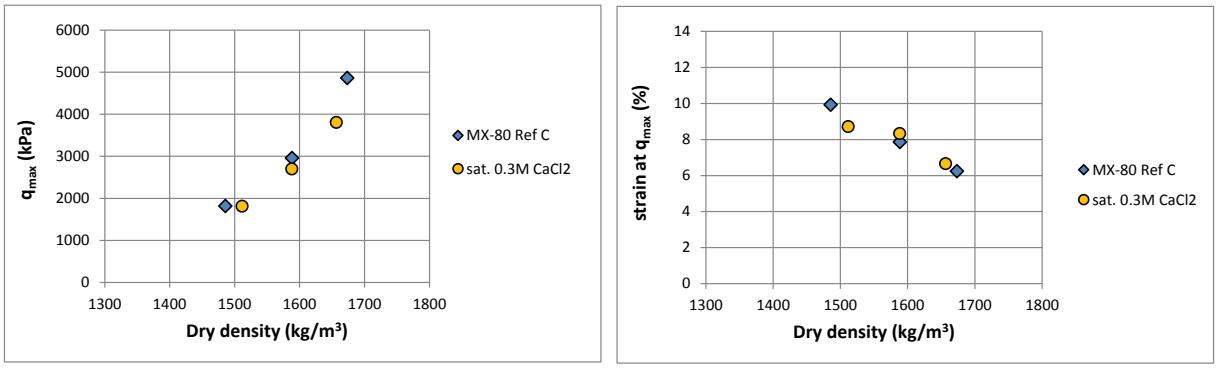

Figure 4-3. Maximum deviator stress q_{max} and corresponding strain ε as a function dry density from test series C.

D. Influence of introduced fractures

In this series specimens were saturated in the saturation device and after 45 days the specimens were dismantled. In seven of the ten specimens a fracture along the specimen and inclined 45°, was introduced. All specimens were then again put into the saturation device with water supply during additional 63 days. The results in *Figure 4-4* show influence both regarding maximum deviator stress and strain compared to the reference specimens (label: MX-80 Ref D).

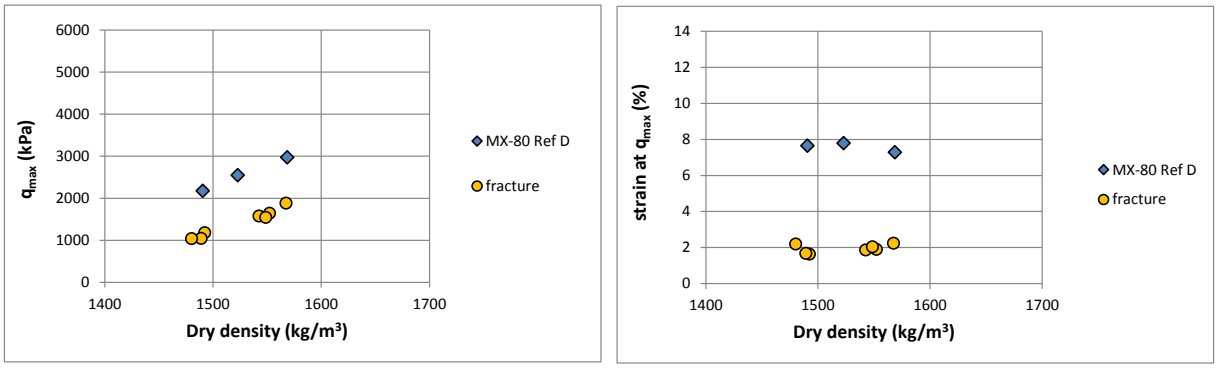

Figure 4-4. Maximum deviator stress q_{max} and corresponding strain ε as a function dry density from test series D.

E. Influence of circulation with Na_2SO_4

In an attempt to enrich MX-80 specimens with additional sodium a solution of 1M Na_2SO_4 was circulated at regular intervals above and under three of the six specimens in this series during 140 days after saturation with de-ionized water. In parallel only de-ionized water was used for the other three specimens (label: MX-80 Ref E). Compared to the specimens only exposed to de-ionized water a slight decrease in maximum deviator stress at failure and a slight increase in strain are seen in the results in *Figure 4-5*.

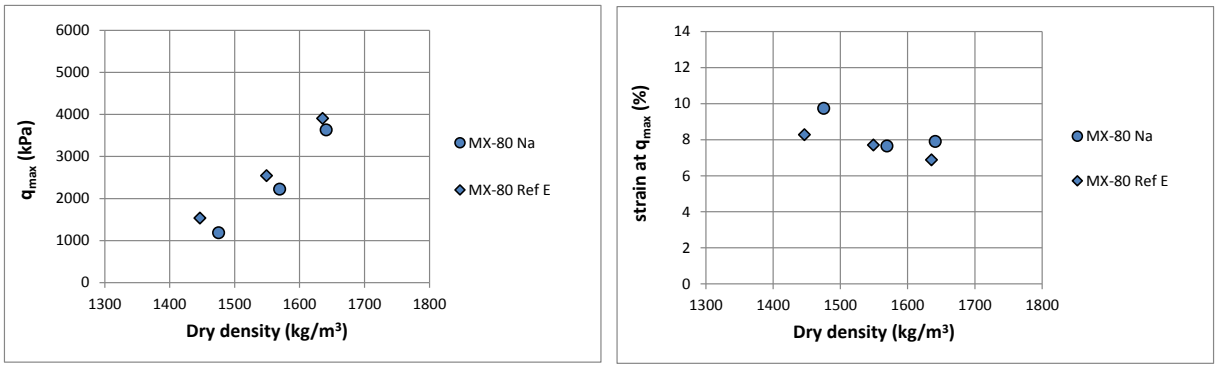

Figure 4-5. Maximum deviator stress q_{max} and corresponding strain ε as a function dry density from test series E.

F. Influence of washing

The influence of washing, i.e. contact with larger volume of water than necessary for the saturation, was studied in this series. The following steps were included in this treatment; pouring MX-80 powder

into de-ionized water, stirring the suspension, evaporating the water and finally grinding the dry material. Some specimens were, in addition, prepared by removal of coarser material where mainly accessory minerals larger than 2 μm was removed and leaving the fine fraction of the material. The saturation was in this series made during 42 days.

From the results in *Figure 4-6* it is shown that two of the three washed specimens (yellow circles) do not show any deviation from the reference specimens (label: MX-80 Ref F) while the third specimen shows higher maximum deviator stress and lower strain at failure. It is also shown that the separation of coarser material, i.e. only using the fine fraction of the material (red circles) gives higher deviator stress and lower strain at failure which was also seen in the results from the similar treated specimens in series B.

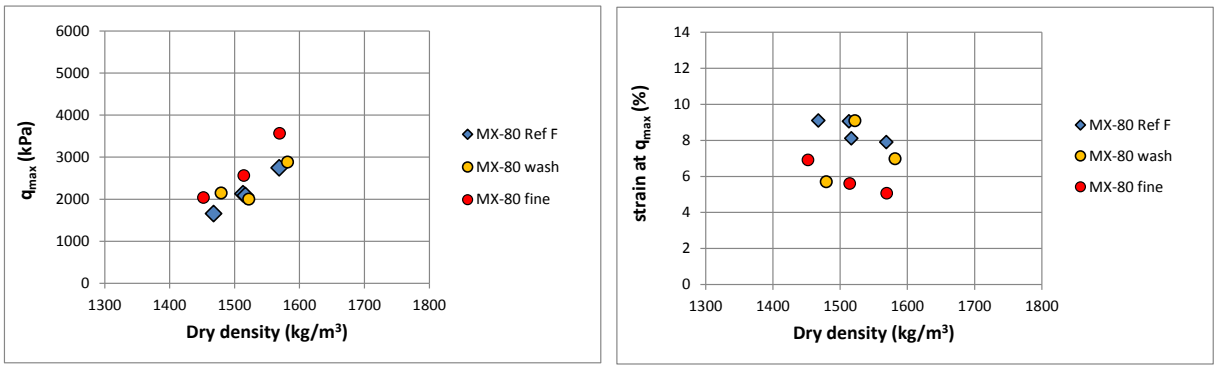

Figure 4-6. Maximum deviator stress q_{max} and corresponding strain ε as a function dry density from test series F.

G. Influence of content of $CaSO_4$

Gypsum (anhydrite) $CaSO_4$ was added to the MX-80 powder used for two specimens in this series and a mass corresponding to 2% of the dry mass of MX-80, was added. De-ionized water was added to the specimens by circulation at regular intervals and the specimens were water supplied during 75 days. One of the specimens were then exposed to 150°C and after that the specimens were water supplied during additional 358 days.

The heated specimen with $CaSO_4$ was brittle and already before shearing the specimen fell in two parts which probably caused the results with lower maximum deviator stress and less strain at failure compared to the results from the not heated specimen but containing $CaSO_4$, shown in *Figure 4-7*.

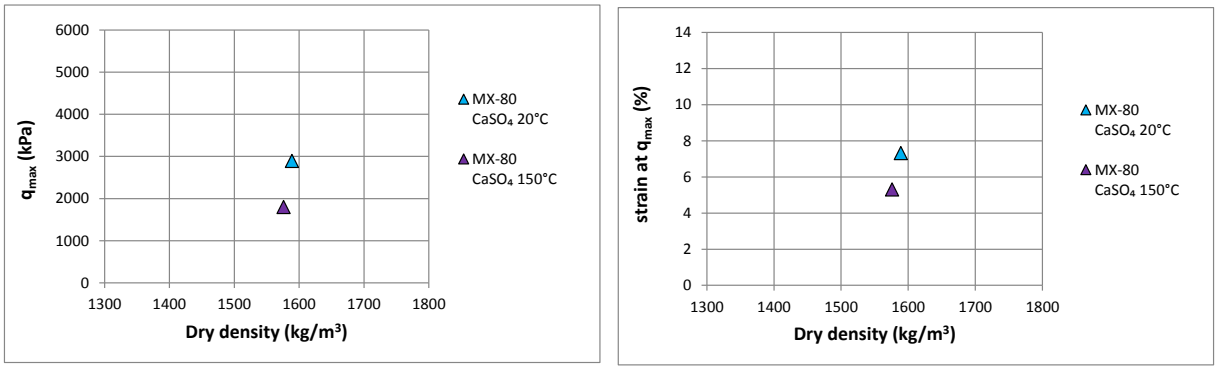

Figure 4-7. Maximum deviator stress q_{max} and corresponding strain ε as a function dry density from test series G.

H. Influence of direction of compaction

In this series all specimens were trimmed from larger compacted specimens. Samples were taken in either the same direction as the direction of compaction (axial direction) or perpendicular to the direction of compaction. After trimming the specimens were put into the saturation device where they were water supplied.

No large difference is seen between specimens sampled in the same or in the perpendicular direction compared to the direction of compaction, see *Figure 4-8*.

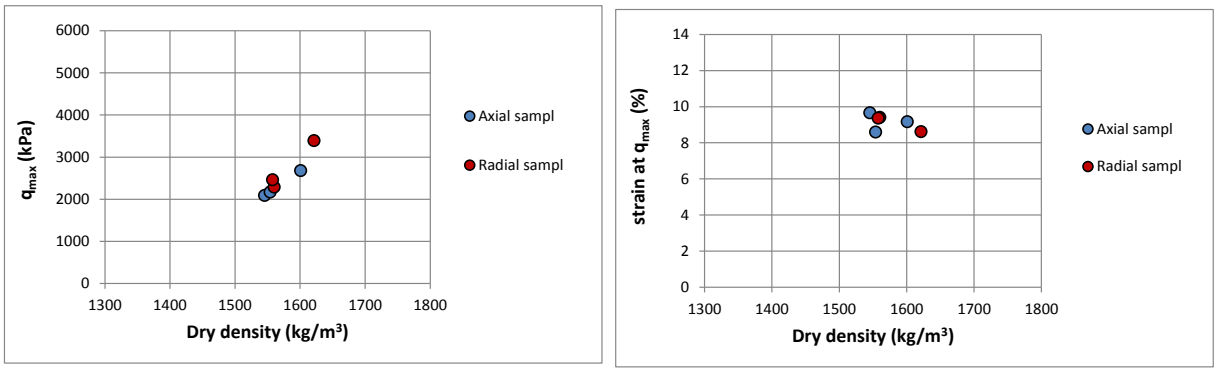

Figure 4-8. Maximum deviator stress q_{max} and corresponding strain ε as a function dry density from test series H.

I. Check of variability

The variability was checked in this series where ten specimens were prepared in the same way. A water pressure of approximately 2 kPa was used for the saturation which was made during 17 days. The results are shown in *Figure 4-9* and compared with the results of all other reference specimens of MX-80 tested in this study.

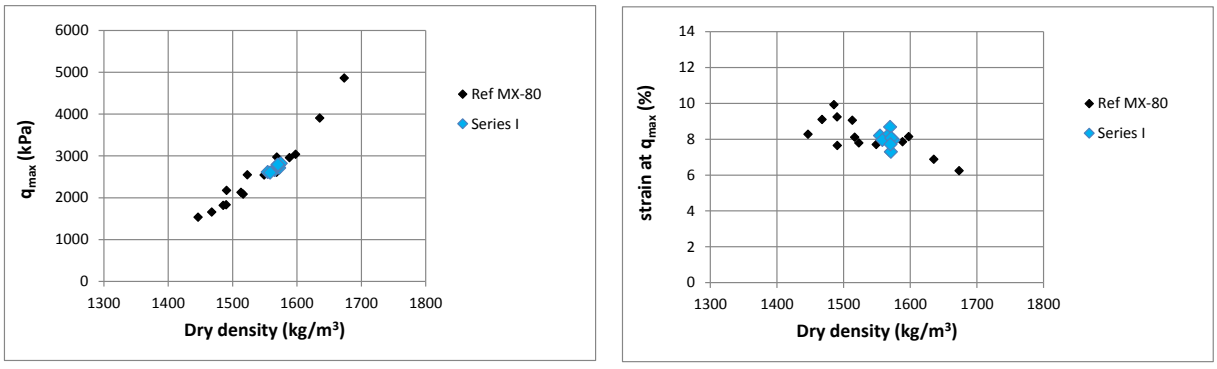

Figure 4-9. Maximum deviator stress q_{max} and corresponding strain ε as a function dry density from series I plotted with all reference specimens.

K-N. Influence of increased temperature on MX-80 and FEBEX

In series K-N the influence of increased temperature on MX-80 and FEBEX bentonites was studied by exposing specimens to short-term heating during 24h in a laboratory oven before the actual tests. The

heating was made either before full saturation (series K and M) or after saturation (series L and N). A controlled water pressure was applied to the specimens heated after saturation which were not the case for the specimens heated before full saturation. The specimens heated before saturation were water supplied during a couple of minutes and after that the device was sealed off and exposed to the increased temperature. The two different conditions present at the heat exposure are in the legends below denominated *(s)* and (*u)*, respectively. The MX-80 specimens were exposed to 90°C, 120°C or 150°C while the FEBEX specimens were only exposed to 90°C.

Unconfined compression tests

Results from the MX-80 specimens exposed to 90°C, 120°C or 150°C are shown in *Figure 4-10* with all non-heated MX-80 references from series A-I. No large deviations are seen in q_{max} while clear deviations in ε are seen on specimens heated to 150°C.

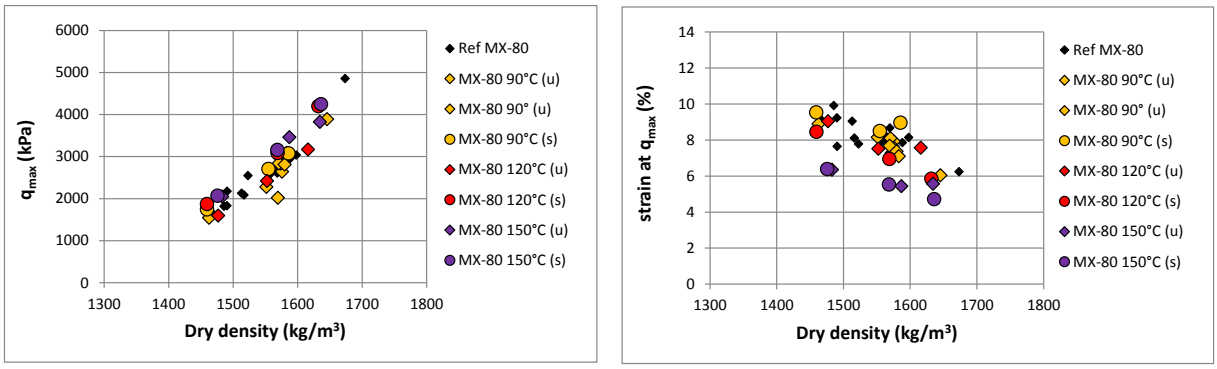

Figure 4-10. Maximum deviator stress q_{max} and corresponding strain ε as a function dry density from test series K and L where MX-80 specimens were exposed to 90°C, 120°C or 150°C. All reference tests are also shown.

Results from the FEBEX specimens exposed to 90°C are shown in *Figure 4-11* together with non-heated FEBEX reference specimens. No large deviations are seen in q_{max} and ε.

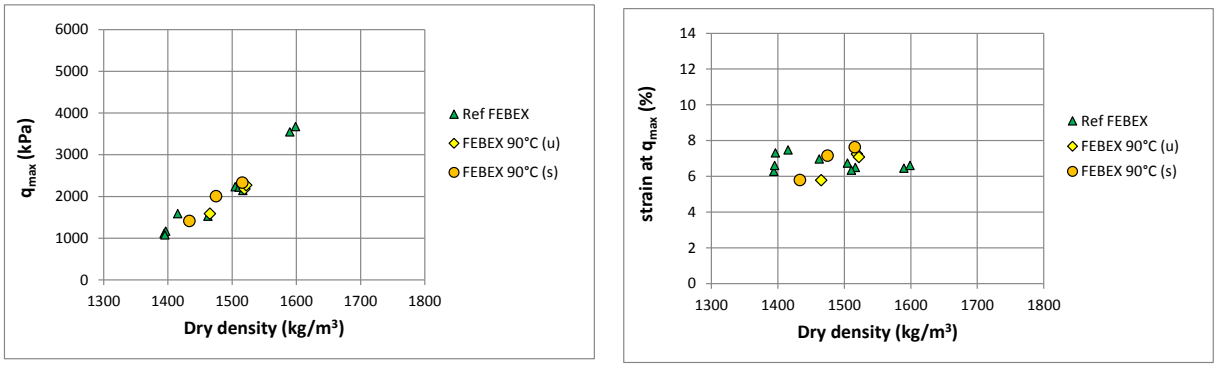

Figure 4-11. Maximum deviator stress q_{max} and corresponding strain ε as a function dry density from test series M and N where FEBEX specimens were exposed to 90°C. Reference specimens are also shown.

Swelling pressure and hydraulic conductivity tests

In *Figure 4-12* all determinations of swelling pressure and hydraulic conductivity of MX-80 specimens heated to 90°C, 120°C or 150°C are shown together with results from the non-heated reference specimens. The swelling pressure was measured with the method described in section 2.5 or evaluated from measurements of *RH*. Compared to the results from the reference specimens no large

deviations are seen in the measured swelling pressures and hydraulic conductivities of heated specimens.

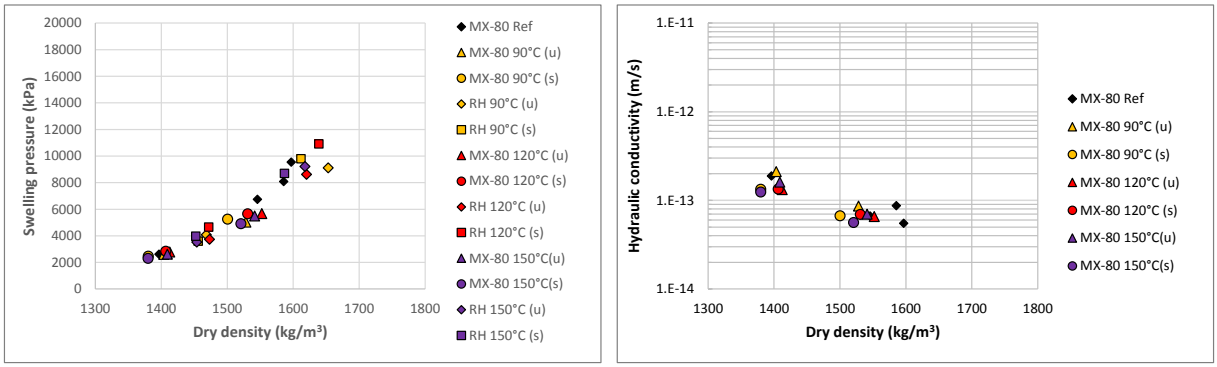

Figure 4-12. Swelling pressure P_s and hydraulic conductivity k_w as a function of dry density from test series K and L where MX-80 specimens were exposed to 90°C, 120°C or 150°C. Reference tests are also shown.

In *Figure 4-13* swelling pressure and hydraulic conductivity of FEBEX specimens heated to 90°C are shown with results from the non-heated reference specimens. The swelling pressure was measured in the same ways as for the MX-80 specimens. No large deviations are seen in the measured swelling pressures and hydraulic conductivities of the heated specimens compared to reference specimens.

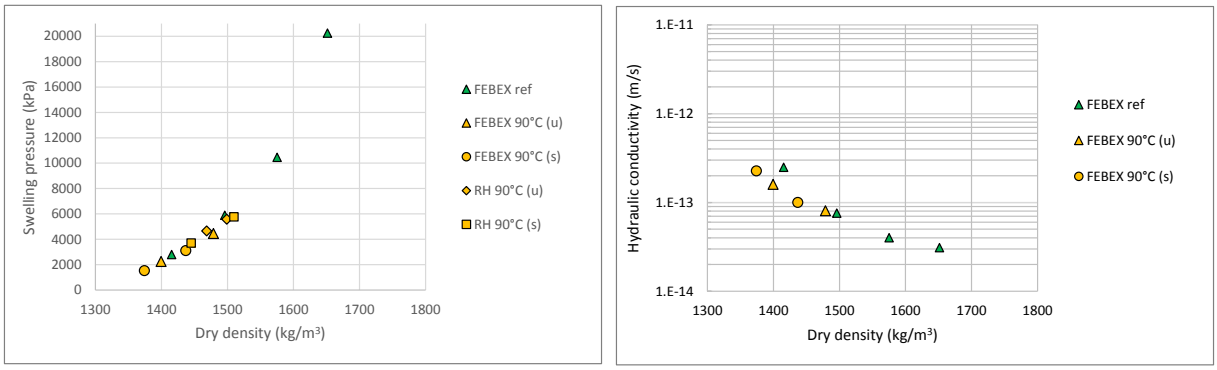

Figure 4-13. Swelling pressure P_s and hydraulic conductivity k_w as a function of dry density from test series M and N where FEBEX specimens were exposed to 90°C. Reference tests are also shown.

5 Analysis

5.1 General

From the reference tests best fit lines were determined for the maximum deviator stress, the corresponding strain, the swelling pressure and the hydraulic conductivity of MX-80 and FEBEX bentonites. For each of the analysed parameter the standard deviation was calculated from the relative differences between measured values of the reference specimens and values corresponding to the best fit line. Each diagram in this chapter contains the best fit line of the corresponding reference specimens plotted in the valid dry density interval. In addition, limiting lines are plotted on each side of the best fit line which correspond to ± 2 times the standard deviation of the relative differences according to above. In the interpretation below deviations are defined as significant when the results from all specimens treated in a specific way are laying outside the limiting lines. The equations of the best fit lines and the standard deviations are given in Appendix A2 where they are further used for interpretation of the influence of short-term heating.

5.2 Reference tests

5.2.1 Maximum deviator stress and corresponding strain

In this study a total of 26 MX-80 reference specimens and 10 FEBEX reference specimens were used for the unconfined compression tests. The test results are shown in *Figure 5-1* and *Figure 5-2* where the evaluated best fit lines and the limiting lines (dotted lines corresponding to ± 2 times the standard deviation of the relative differences) are shown.

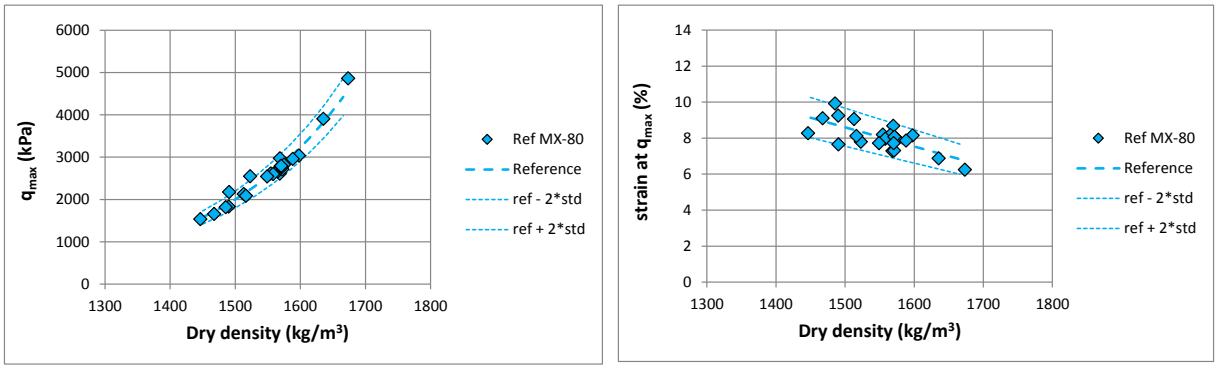

*Figure 5-1. Results from the MX-80 reference specimens used in this study are plotted as maximum deviator stress and corresponding strain as a function of dry density. The labels Reference and ref±2*std denote the best fit lines and lines representing ± 2 times the standard deviations.*

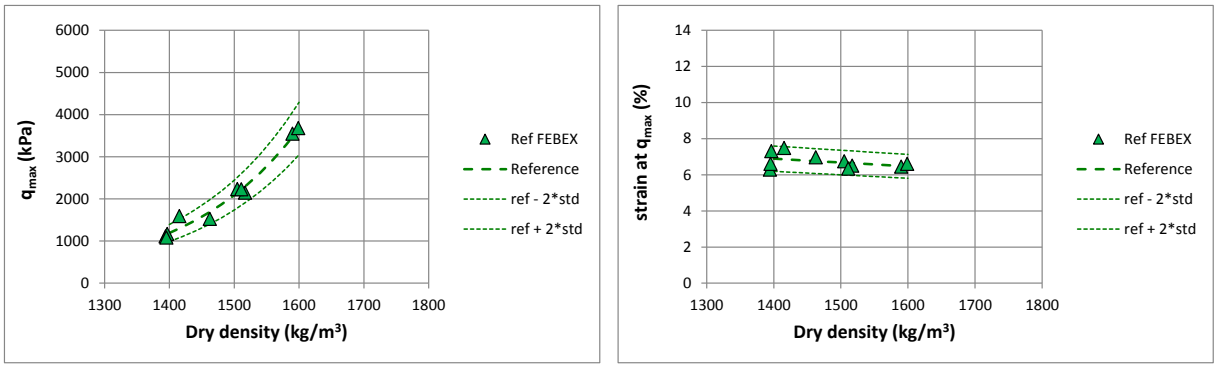

*Figure 5-2. Results from the FEBEX reference specimens used in this study are plotted as maximum deviator stress and corresponding strain as a function of dry density. The labels Reference and ref±2*std denote the best fit lines and lines representing ± 2 times the standard deviations.*

5.2.2 Swelling pressure and hydraulic conductivity

In this study four MX-80 reference specimens and four FEBEX reference specimens were tested with the swelling pressure and hydraulic conductivity test. The test results are shown in *Figure 5-3* and *Figure 5-4* together with the best fit lines and the limiting (dotted) lines. In addition, relationships from other studies (Åkesson et al., 2010, Börgesson et al., 1995, Villar, 2002) are also shown.

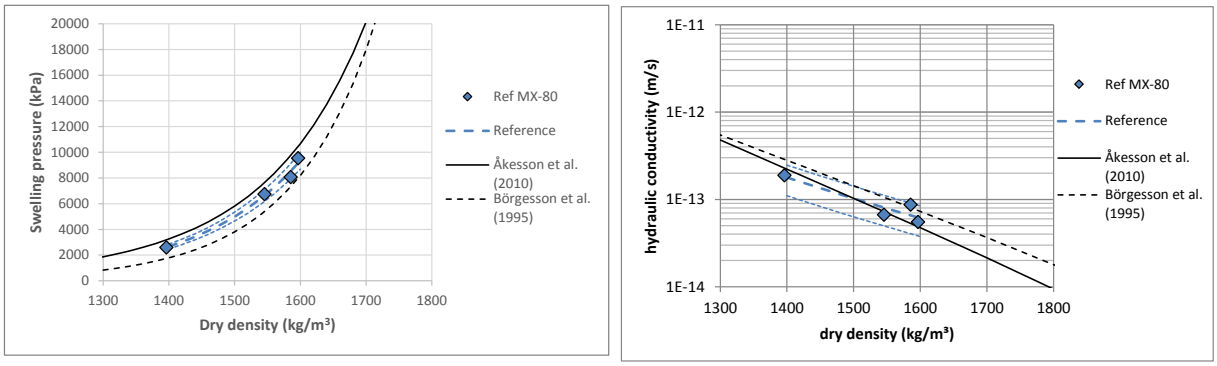

Figure 5-3. Results from MX-80 reference specimens tested in this study are plotted as swelling pressure and hydraulic conductivity as a function of dry density. The labels Reference denote the best fit lines and the lines representing the best fit lines ± 2 times the standard deviations are also shown (blue dotted lines). In addition, relations from other studies are shown (Åkesson et al., 2010, Börgesson et al., 1995).

The swelling pressure and hydraulic conductivity of MX-80 specimens measured in this study correspond well with previous measured values shown in Figure 5-3. The hydraulic conductivity of FEBEX specimens, to the right in Figure 5-4, also corresponds well with previous measured values. However, regarding the swelling pressure of FEBEX specimens, to the left in *Figure 5-4*, a deviation between measurements in this study and previous measurements is seen in the upper range of dry density and the reason for this is not clear.

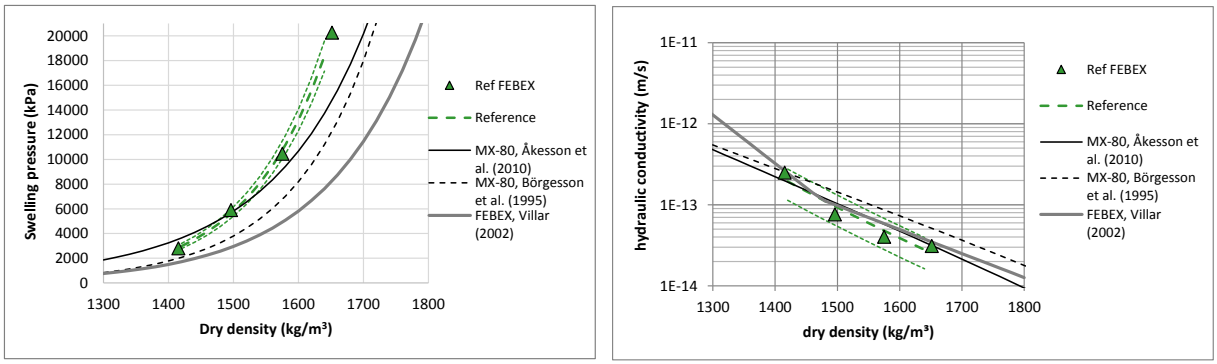

Figure 5-4. Results from FEBEX reference specimens tested in this study are plotted as swelling pressure and hydraulic conductivity as a function of dry density. The labels Reference denote the best fit lines and the best fit lines ± 2 times the standard deviations are also shown (green dotted lines). In addition, results from other studies are shown (Åkesson et al., 2010, Börgesson et al., 1995, Villar, 2002)

5.3 Influence of short-term heating on specimens of MX-80 and FEBEX

5.3.1 General

The test series where influence of increased temperature were studied included both unconfined compression tests and the combined swelling pressure - hydraulic conductivity tests. Additional analysis of the influence of increased temperature is given in Appendix A2. As mentioned above the labels (*s)* and (*u)* are used for the specimen being heated after and before full saturation, respectively.

Below, the deviations seen in the test results of some of the specimens compared to references were directly correlated to the maximum temperatures of the short time exposure although the quantification of the influence was made after the heat exposure and not during the exposure.

5.3.2 Maximum deviator stress and corresponding strain

In *Figure 5-5* and *Figure 5-6* the results from *Figure 4-10* and *Figure 4-11* are shown with the corresponding best fit lines.

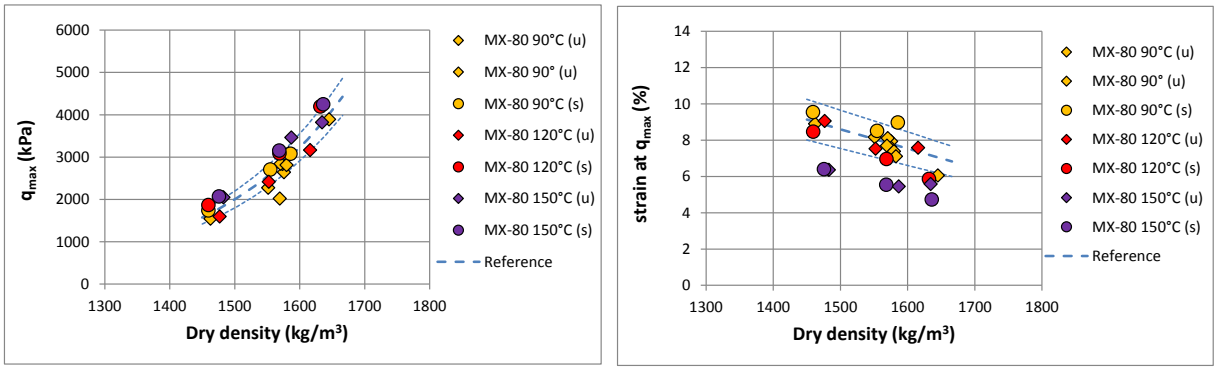

Figure 5-5. Maximum deviator stress and corresponding strain as a function of dry density from Figure 4-10 and the best fit lines of the MX-80 references.

All MX-80 specimens heated after saturation show a slightly higher q_{max} compared to the reference line. On these specimens a tendency to increased q_{max} and decreased strain at failure with increased temperature are also seen. A scatter is seen on the test results from the specimens heated before saturation but consistency between results from the two types of heating is seen on specimens heated to 150°C. Significant deviations are seen on q_{max} from specimens heated to 120°C and 150°C after saturation and on ε from all specimens heated to 150°C.

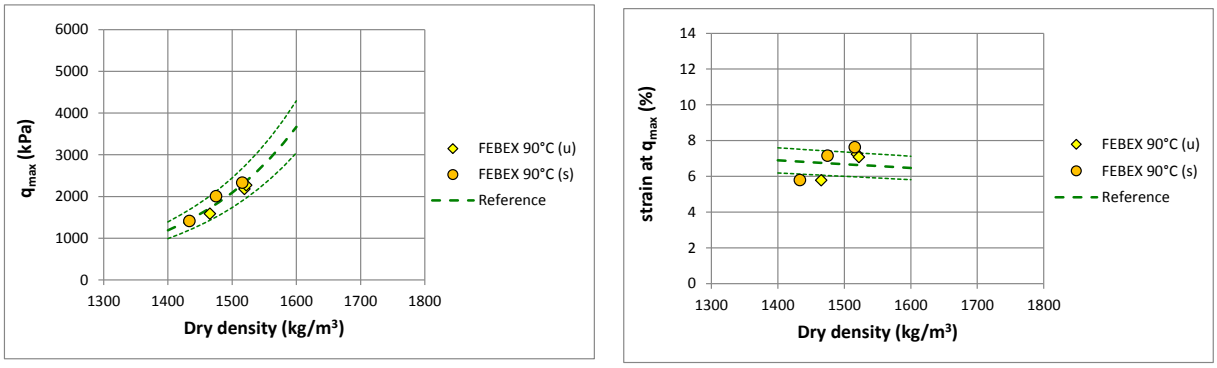

Figure 5-6. Maximum deviator stress and corresponding strain as a function of dry density from Figure 4-11 and the best fit lines of the FEBEX references.

In the results from the FEBEX specimens heated to 90°C the deviations from the best fit line of q_{max} are small. Regarding the strain ε the scatter is large and no significant deviation is seen.

5.3.3 Swelling pressure and hydraulic conductivity

The majority of the measured swelling pressures and hydraulic conductivities of heated MX-80 specimens is lower than the references. A tendency to larger effect the larger temperature is only seen on the swelling pressure measured on specimens heated after full saturation. The deviations are small and the only deviation that can be considered as significant, according to the definition above, is the hydraulic conductivity measured on specimens heated to 150°C after saturation.

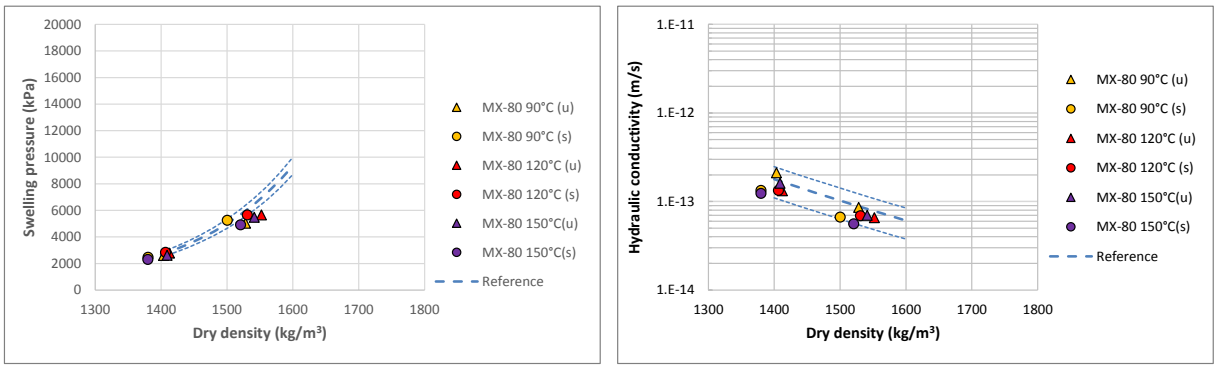

Figure 5-7. Swelling pressure and hydraulic conductivity as a function of dry density from Figure 4-12 and the best fit lines of the MX-80 references. The shown swelling pressures were all determined with the method described in section 2.5.

The results of the heat exposed FEBEX specimens show lower values than the references both regarding swelling pressure and hydraulic conductivity. The deviations are small and the only significant deviations, according to the definition above, are the swelling pressures measured on specimens heated after saturation to 90°C, estimated from extrapolation of the reference lines.

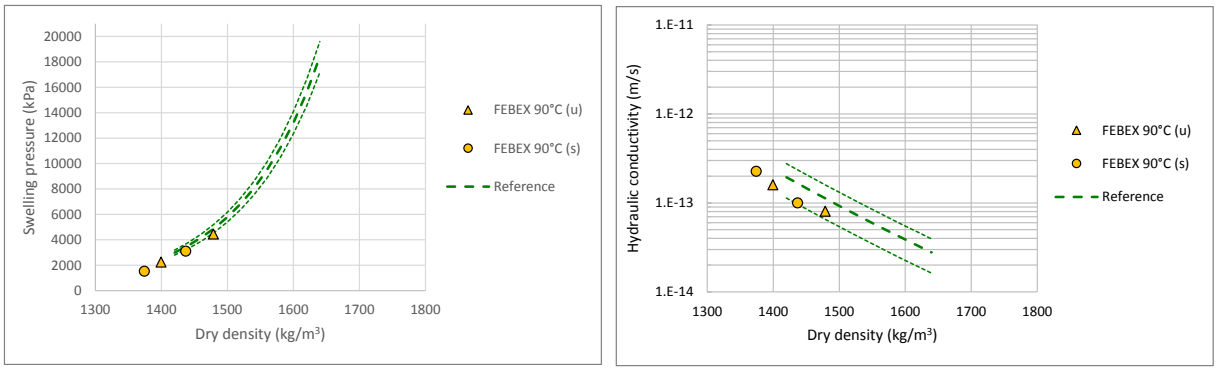

Figure 5-8. Swelling pressure and hydraulic conductivity as a function of dry density from Figure 4-13 with the best fit lines of the FEBEX references. The swelling pressures were all determined with the method described in section 2.5.

5.3.4 Discussion

In addition to the influence of short-term heating on e.g. the stress-strain- property discussed above, also the degree of saturation can be analysed. The specimens were supposed to be fully saturated at the determination of swelling pressure and the necessary time for the saturation was set to eight days for the dimension used. However, longer time periods were used in some series and when results from different series were compared small differences in the degrees of saturation were seen. In *Figure 5-9* the degree of saturation of MX-80 specimens, determined after the swelling pressure and hydraulic conductivity test, are shown. Each circle and diamond are the average of two specimens and the blue square with the label "MX-80 20" is an average of the four reference specimens.

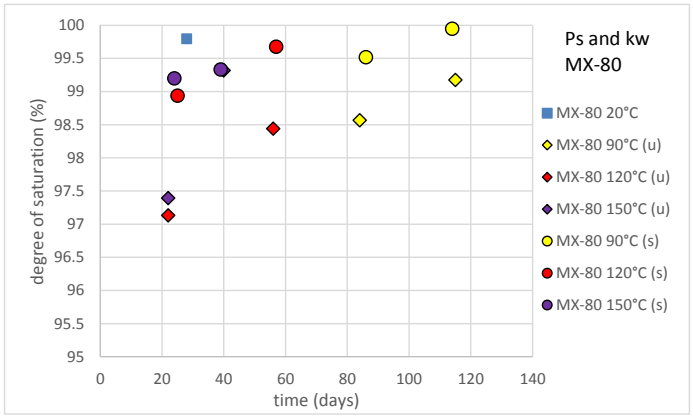

Figure 5-9. Degree of saturation of MX-80 specimens from the swelling pressure and hydraulic conductivity tests from series K and L where the specimens were exposed to heat. Each point is an average of two or four specimens. The height of the specimens was 10 mm.

In the diagram the circles and diamonds are test results from specimens exposed to heat and the colours (yellow, red, purple) show the temperature used (90°C, 120°C, 150°C) and the markers (diamond, circle) show when and how the specimens were exposed to increased temperature (before full saturation without controlled water pressure, after full saturation with controlled water pressure). It can be seen that the specimens exposed to heat needed longer time than the reference specimens to be fully saturated. In addition, the specimens heated before full saturation (diamonds) seemed to need longer time to saturation than specimens heated after saturation (circles). However, the specimens shown in *Figure 5-9* were regarded as saturated in the interpretation. In this study, all specimens were interpreted as being saturated although some of the FEBEX specimens had a degree of saturation as low as 92%. The actual specimens were tested with the unconfined compression test and from

previous studies with this method no influence of such value of degree of saturation was seen on the deviator stress at failure while the strain at failure may be lower compared to fully saturated specimens (Dueck, 2010).

5.4 Impacts from other factors studied

5.4.1 Influence of different an-ions

Some specimens in the series B and F were prepared by removing the coarser fractions of MX-80, larger than 2 μm. Since this procedure is also necessary for the production of the purified WyNa the effect of the ion exchange, only, can be evaluated from *Figure 5-10*. The Na dominated WyNa has a somewhat lower deviator stress at failure but almost the same strain at failure compared to the MX-80 specimens with the coarser material removed. The reference lines of MX-80 are also shown in the diagrams.

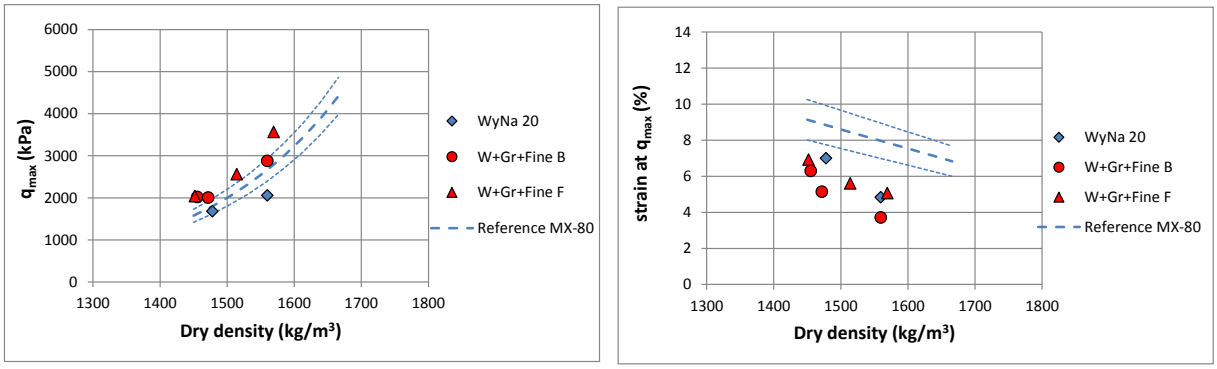

Figure 5-10. Maximum deviator stress and corresponding strain as a function of dry density. Selected results from series A, B and F. The MX-80 reference lines are also shown.

Regarding the purified ion exchanged Na bentonite WyNa some of these specimens were heated to 150°C and compared to the non-heated specimens of WyNa the heated specimens have somewhat higher deviator stress and decreased strain at failure according to *Figure 5-11*. In the diagrams the results from this study are presented with results from previous studies shown with triangles (Dueck et al., 2010, Dueck, 2010) which agree regarding q_{max} but where the influence of heat on strain at failure ε is ambiguous.

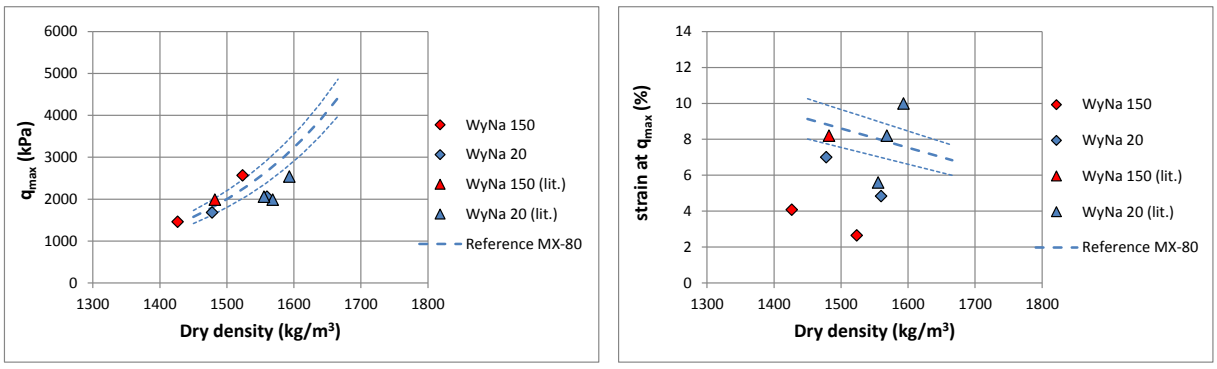

Figure 5-11. Maximum deviator stress and corresponding strain as a function of dry density. Selected results from series A, B and F and results from Dueck (2010) and Dueck et al. (2010). The results from previous studies are marked with (lit) in the legend.

In two other series solutions of $CaCl_2$ and Na_2SO_4 were contacted with MX-80 specimens. In series C 0.3M $CaCl_2$ was circulated at regular intervals during 40 days and in series E a solution of 1M Na_2SO_4 was introduced after saturation with de-ionized water and then circulated at regular intervals during approximately 140 days. The results from both treatments resulted in small decreases in q_{max} but no significant deviations are seen in *Figure 5-12*.

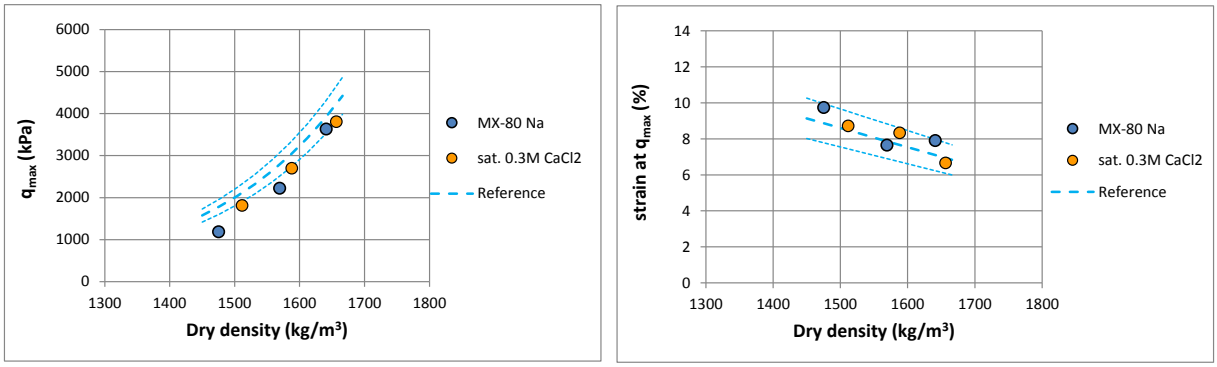

Figure 5-12. Maximum deviator stress and corresponding strain as a function of dry density. Selected results from series C and E with MX-80 reference lines.

In a series, series G, content of $CaSO_4$ was added to two specimens and one of the specimens were exposed to short-term heating to 150°C. Decreased deviator stress and strain at failure were measured. However, from similar tests in a previous study decreased strain was seen but not decreased deviator stress at failure (Dueck, 2010).

5.4.2 Influence of preparation technique

The influence of washing and grinding included in some preparation methods can be evaluated from *Figure 5-13* where results from unconfined compression tests on washed and ground MX-80 specimens (yellow circles, from series F) are shown and compared with MX-80 specimens only being ground (yellow triangles, from series B). No influence is seen on the deviator stress but while specimen consisting of ground material show increased strain at failure the specimens consisting of ground and washed material show decreased strain at failure. However, no deviations are considered as significant.

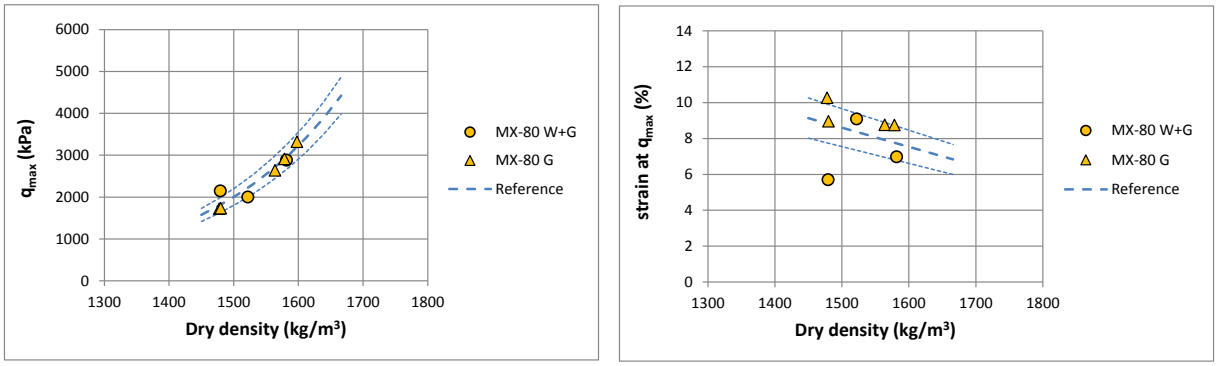

Figure 5-13. Maximum deviator stress and corresponding strain as a function of dry density. Results from series B and F with MX-80 reference lines.

Two additional series were made where the influence of preparation was studied; the introduction of fractures (series D) and different directions of sampling (series H). Results from both series are shown

in *Figure 5-14*. The introduced fractures significantly reduced both the maximum deviator stress q_{max} and the strain at failure ε. Regarding sampling a small decrease in q_{max} and a small increase in ε are seen compared to the reference lines but almost no difference is seen between the two directions of sampling. However, only the deviations of the maximum deviator stress q_{max} from the axially sampled specimens and the strain at failure ε from the radially sampled specimens can be regarded as significant.

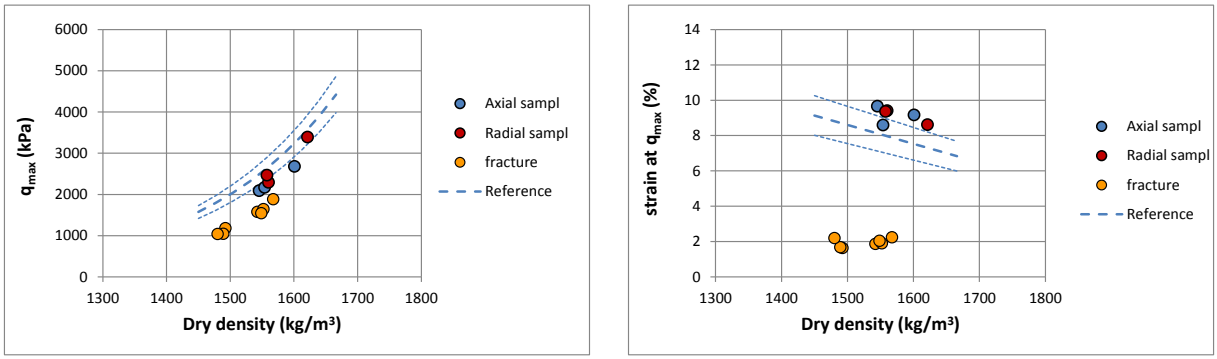

Figure 5-14. Results from tests where fractures were introduced and from tests with specimens sampled from larger specimens, i.e. series D and H with MX-80 reference lines.

5.5 Discussion

A compilation of the main findings from the test series run in this study is shown in Table 5-1 and where deviations considered as significant are marked with the signs + and - which mean increased and decreased values, respectively. In this study deviations were considered as significant only if all results from a test series were laying outside the best fit lines ± 2 times the standard deviation of the relative differences of the reference specimens.

It should be pointed out that that in some series the deviations were interpreted as significant but they were still small and this was the case with sampling in Table 5-1 and regarding the decreased values of swelling pressure and hydraulic conductivity marked with minus signs in Table 5-2.

Table 5-1. Main findings regarding the stress-strain-property from test series made in this study.

From PEBS series	Material	Max Temp.	Significant deviations on		Series
			strength	shear strain	
Influence of grinding	MX-80	20°C	no	no	B
Influence of saturation with CaCl2	MX-80	20°C	no	no	C
Influence of introduced fractures	MX-80	20°C	-	-	D
Influence of circulation with Na2SO4	MX-80	20°C	no	no	E
Influence of washing	MX-80	20°C	no	no	F
Influence of short-term heating with content of CaSO4 added	MX-80+CaSO4	150°C	brittle	brittle	G
Influence of sampling	MX-80	20°C	-	+	H
Influence of direction of sampling	MX-80	20°C	no	no	H
Influence of short-term heating **after** saturation	MX-80	90°C	no	no	L
Influence ofshort-term heating **after** saturation	MX-80	120°C	+	no	L
Influence of short-term heating **after** saturation	MX-80	150°C	+	-	L
Influence of short-term heating **before** saturation	MX-80	90°C	no	no	K
Influence of short-term heating **before** saturation	MX-80	120°C	no	no	K
Influence of short-term heating **before** saturation	MX-80	150°C	no	-	K
Influence of short-term heating **after** saturation	FEBEX	90°	no	no	N
Influence of short-term heating **before** saturation	FEBEX	90°	no	no	M

Table 5-2. Main findings regarding swelling pressure and hydraulic conductivity from test series made in this study.

From PEBS series	Material	Max Temp.	Significant deviations on		Series
			Swelling pr.	Hydr. cond.	
Influence of short-term heating **after** saturation	MX-80	90°C	no	no	L
Influence of short-term heating **after** saturation	MX-80	120°C	no	no	L
Influence ofshort-term heating **after** saturation	MX-80	150°C	no	-	L
Influence of short-term heating **before** saturation	MX-80	90°C	no	no	K
Influence of short-term heating **before** saturation	MX-80	120°C	no	no	K
Influence of short-term heating **before** saturation	MX-80	150°C	no	no	K
Influence of short-term heating **after** saturation	FEBEX	90°	-	no	N
Influence of short-term heating **before** saturation	FEBEX	90°	no	no	M

6 Conclusions

This study was focused on the stress-strain properties of bentonite exposed to increased temperatures but the influence of different mineral composition, different an-ions and different preparation methods were also studied. The influence of the different treatments was quantified by measurements of stresses and strains during the unconfined compression test and from some of the series also by measurements of swelling pressure and hydraulic conductivity.

In the test series with increased temperature the specimens were exposed to short-term heating in a laboratory oven during 24h. Specimens of MX-80 were exposed to 90°C, 120°C and 150°C and specimens of FEBEX were exposed to 90°C. The heating was made both after and before full saturation where heating after full saturation meant heated with a controlled water pressure to a maximum of 600 kPa while heating before full saturation in this study meant heating at a high degree of saturation without control of the water pressure but under sealed conditions.

The following correlations can be seen in the results from this study:

- A tendency of increased deviator stress at failure with increased temperature after short-term heating but significant deviations only after heating to 120°C and 150°C.
- Significant decrease in strain at failure only after short-term heating to 150°C.
- Small decreases in swelling pressure and hydraulic conductivity after short-term heating.
- Significant influence on deviator stress and strain at failure for specimens with old fractures.
- Small but no significant influence on deviator stress and strain at failure after circulation with solutions of $CaCl_2$ or Na_2SO_4.
- No influence on deviator stress and strain at failure of grinding or washing the material at preparation but small influence of sampling.

Acknowledgements

This work was supported by:

- European Atomic Energy Community's Seventh Framework Programme (FP7/2007-2011) under grant agreement n° 249681.
- Swedish Nuclear Fuel and Waste Management Company (SKB).

References

Börgesson L., Johannesson L.-E., Sandén T., Hernelind J., 1995. Modelling of the physical behavior of water saturated clay barriers. Laboratory test, material models and finite element application. SKB Technical Report TR-95-20. Svensk Kärnbränslehantering AB.

Börgesson L., Johannesson L.-E., Hernelind J.; 2004. Earthquake induced rock shear through a deposition hole. Effect on the canister and the buffer. SKB Technical Report TR-04-02.

Dueck A., 2010. Thermo-mechanical cementation effects in bentonite investigated by unconfined compression tests. SKB Technical Report TR-10-41. Svensk Kärnbränslehantering AB.

Dueck A., Börgesson L., 2007. Model suggested for an important part of the hydro-mechanical behavior of a water unsaturated bentonite. Engineering Geology 92, pp.160-169. Elsevier.

Dueck A., Börgesson L., Johannesson L.-E., 2010. Stress-strain relation of bentonite at undrained shear – Laboratory tests to investigate the influence of material composition and test technique. SKB Technical Report TR-10-32. Svensk Kärnbränslehantering AB.

Dueck A., Johannesson L.-E., Kristensson O., Olsson S., Sjöland A., 2011. Hydro-mechanical and chemical-mineralogical analyses of the bentonite buffer from a full-scale field experiment simulating a high-level waste repository. Clays and Clay Minerals 59, 595-607. GeoScienceWorld.

Fredlund D.G., Rahardjo H., 1993. Soil Mechanics for unsaturated soils, John Wiley & Sons Inc., ISBN 0-471-85008-X, Chapter 4.

Greenspan L., 1977. Humidity fixed points of binary saturated aqueous solutions. Journal of research of the national Bureau of Standards, A. Physics and Chemistry, Vol 81A, No 1, pp 89-96.

Kahr G., Kraehenbuehl F., Stoeckli H.F., Műller-Vonmoos M., 1990. Study of the water-bentonite system by vapour adsorption, immersion calorimetry and X-ray techniques: II. Heats of immersion, swelling pressures and thermodynamic properties, Clay Minerals 25, pp 499-506

Karnland O., Muurinen A., Karlsson F., 2005. Bentonite swelling pressure in NaCl solutions – Experimentally determined data and model calculations. Advances in understanding engineered clay barriers. Proceedings of the international symposium on large scale tests in granite, Edited by Alonso E.E. and Ledesma A. A.A. Balkema Publisher.

Karnland O., Olsson S., Nilsson U., 2006. Mineralogy and sealing properties of various bentonites and smectite-rich clay minerals. SKB Technical Report TR-06-30. Svensk Kärnbränslehantering AB.

Karnland O., Olsson S., Dueck A., Birgersson M., Nilsson U., Hernan-Håkansson T., Pedersen K., Nilsson S., Eriksen T., Rosborg B., 2009. Long term test of buffer material at the Äspö Hard Rock Laboratory, LOT project. Final report on the A2 test parcel. SKB Technical Report TR-09-29. Svenska Kärnbränslehantering AB.

PEBS, 2010. Long-term performance of Engineered Barrier Systems (PEBS), Annex I – "Description of Work", Seventh Framework Programme, European Commission.

Svensson D., Dueck A., Nilsson U., Olsson S., Sandén T., Lydmark S., Jägerwall S., Pedersen K., Hansen S., 2011. Alternative Buffer Material, Status of the ongoing laboratory investigation of reference materials and test package 1. SKB Technical Report TR-11-06. Svenska Kärnbränslehantering AB.

Villar M.V., 2002. Thermo-hydro-mechanical characterisation of a bentonite from Cabo de Gata. A study applied to the use of bentonite as sealing material in high level radioactive waste repositoties. ENRESA technical publication 04/2002.

Wadsö L., Svennberg K., Dueck A., 2004. An experimentally simple method for measuring sorption isotherms. Drying Technology 22(10): 2427-2440.

Åkesson M., Börgesson L., Kristensson O., 2010. Sr-Site Data report, THM modelling of buffer, backfill and other system components. SKB TR-10-44. Svensk kärnbränslehantering AB.

Åkesson M., Olsson S., Dueck A., Nilsson U., Karnland O., Kiviranta, L., Kumpulainen S., Lindén J., 2012. Temperature buffer test. Hydro-mechanical and chemical/mineralogical characterizations. SKB Report P-12-06. Svenska Kärnbränslehantering AB.

Appendices

A1 Test results

A1.1 Diagrams

A1.1.1 Deviator stress as a function of strain at shear

In the diagrams the test series is used as title and in the legend the labels of each specimens contain Test ID and the dry density (kg/m^3).

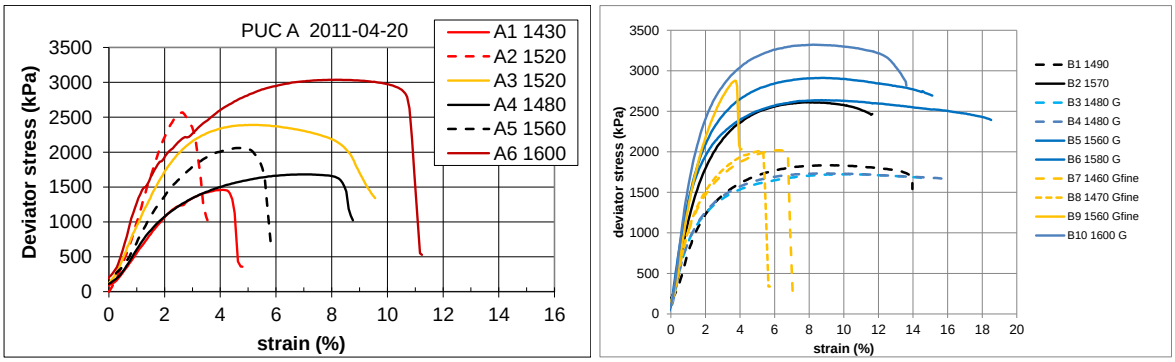

Figure A1-1. Results from unconfined compression tests on specimens in series A and B.

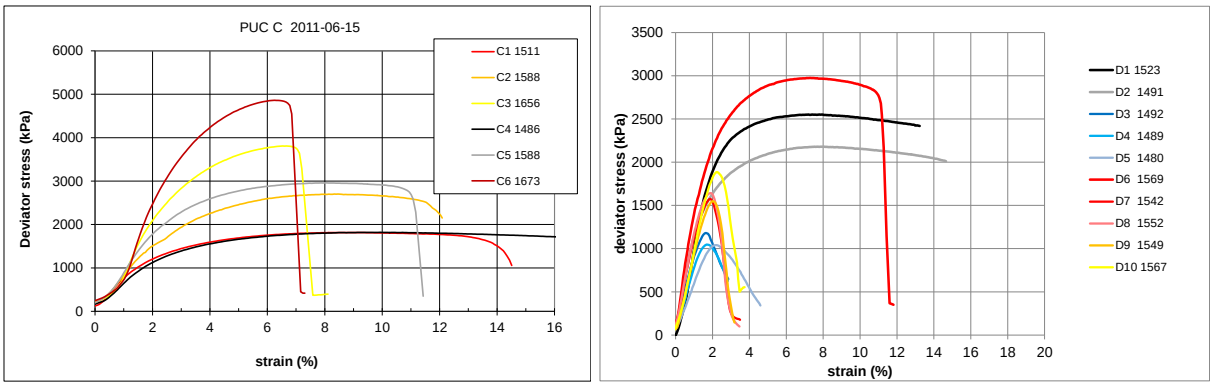

Figure A1-2. Results from unconfined compression tests on specimens in series C and D.

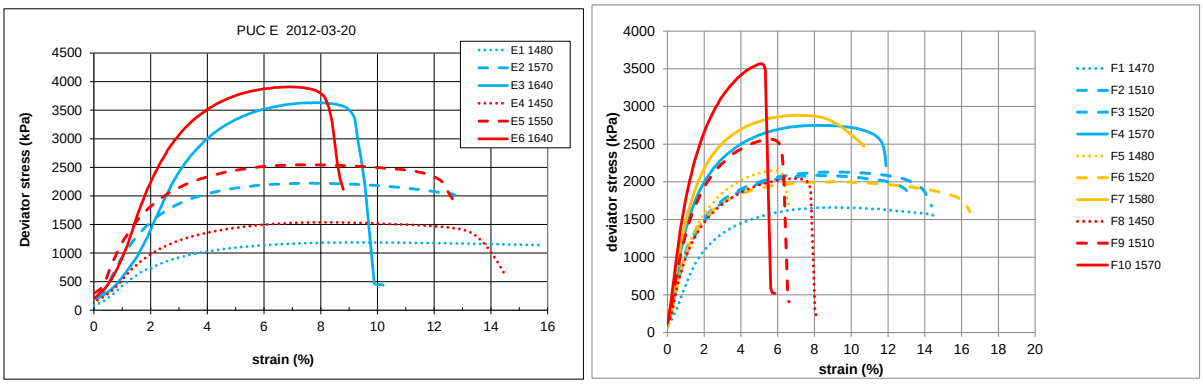

Figure A1-3. Results from unconfined compression tests on specimens in series E and F.

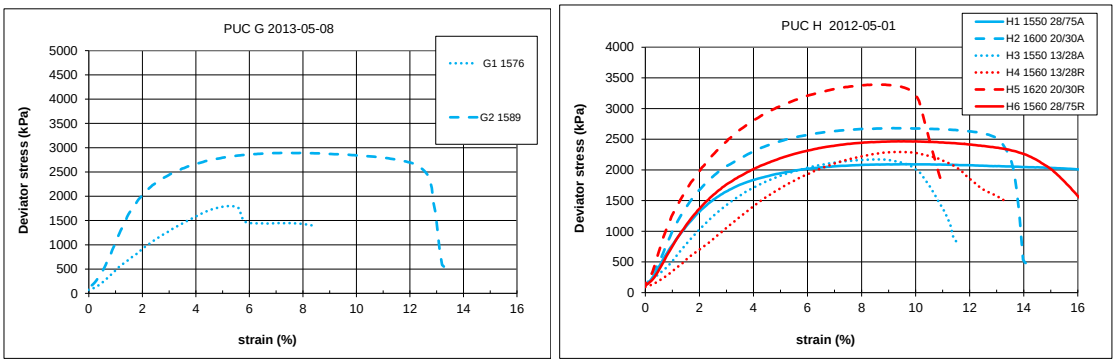

Figure A1-4. Results from unconfined compression tests on specimens in series G and H.

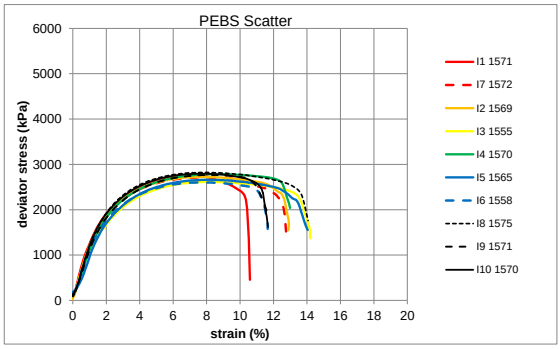

Figure A1-5. Results from unconfined compression tests on specimens in series I.

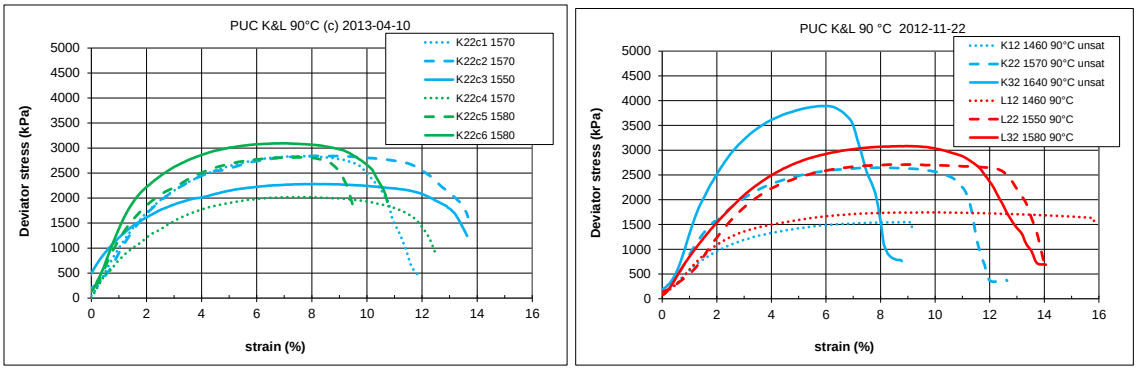

Figure A1-6. Results from unconfined compression tests on specimens exposed to 90°C in series K&L.

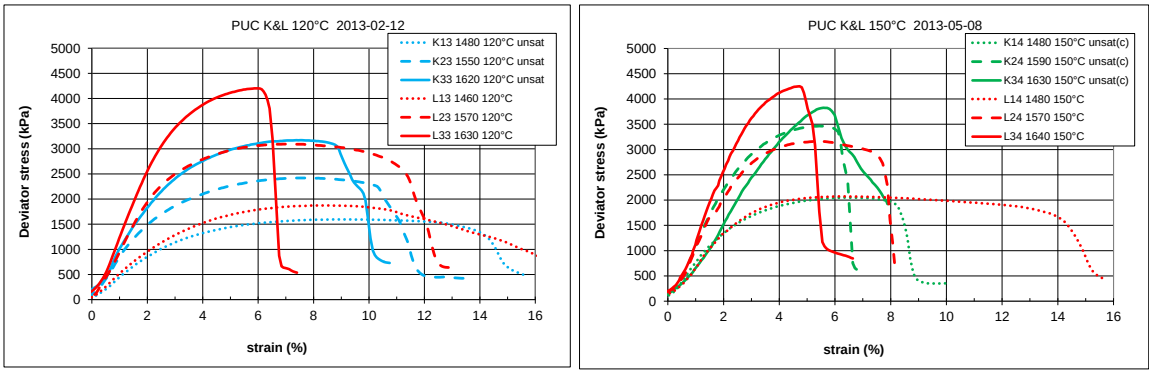

Figure A1-7. Results from unconfined compression tests on specimens exposed to 120°C and 150°C in series K&L.

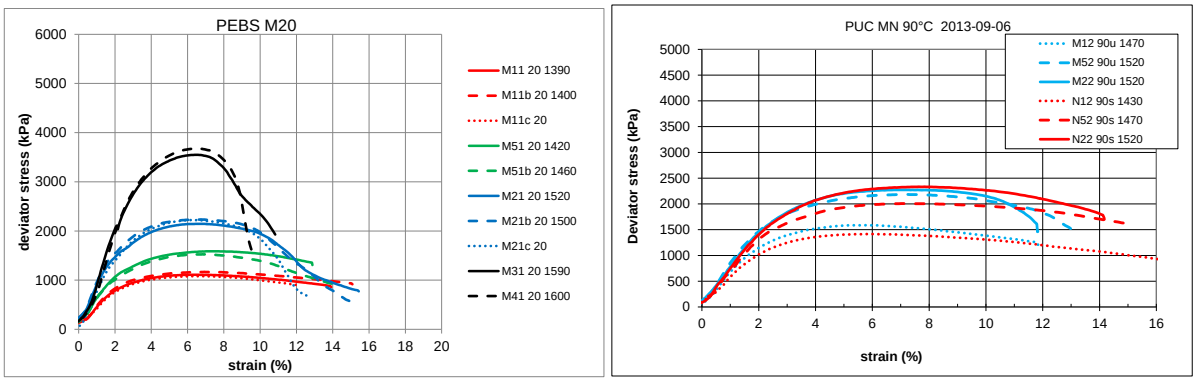

Figure A1-8. Results from unconfined compression tests on specimens exposed to 90°C in series M&N.

A1.1.2 Evolution of swelling pressure

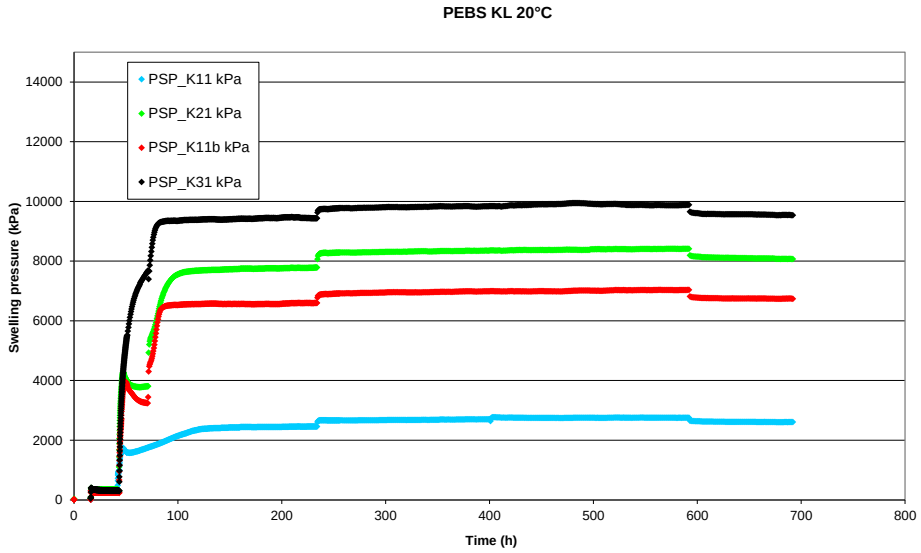

Figure A1-9. Evolution of swelling pressure of reference specimens in series K.

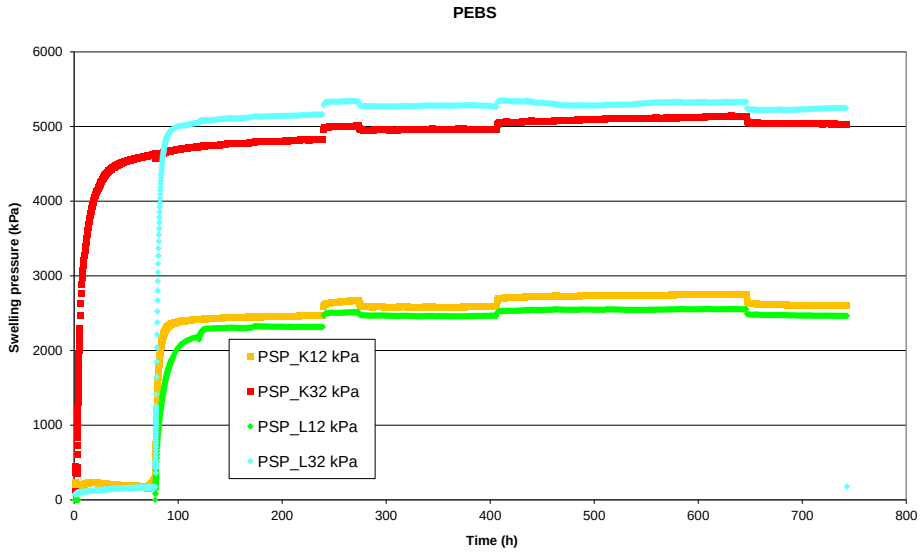

Figure A1-10. Evolution of swelling pressure of specimens exposed to 90°C in series K&L.

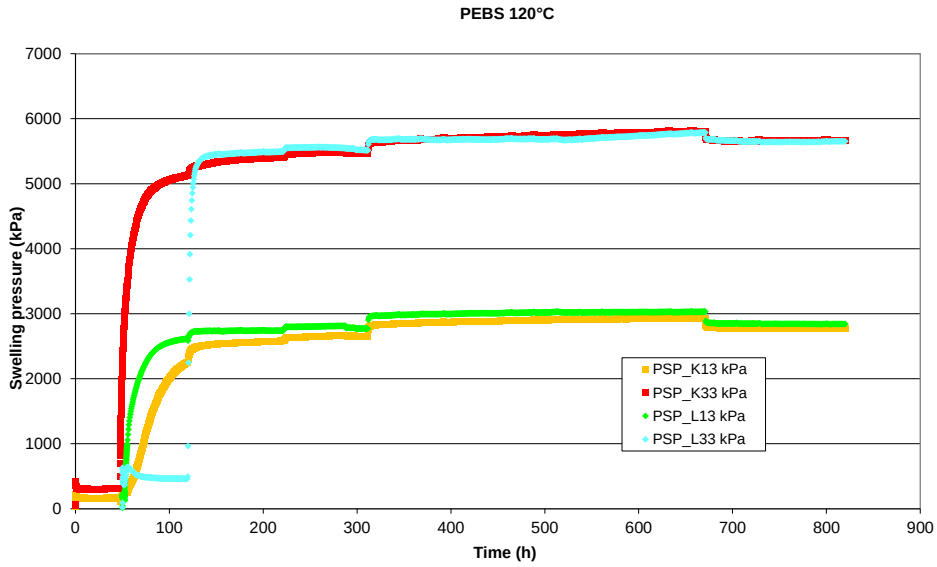

Figure A1-11. Evolution of swelling pressure of specimens exposed to 120°C in series K&L.

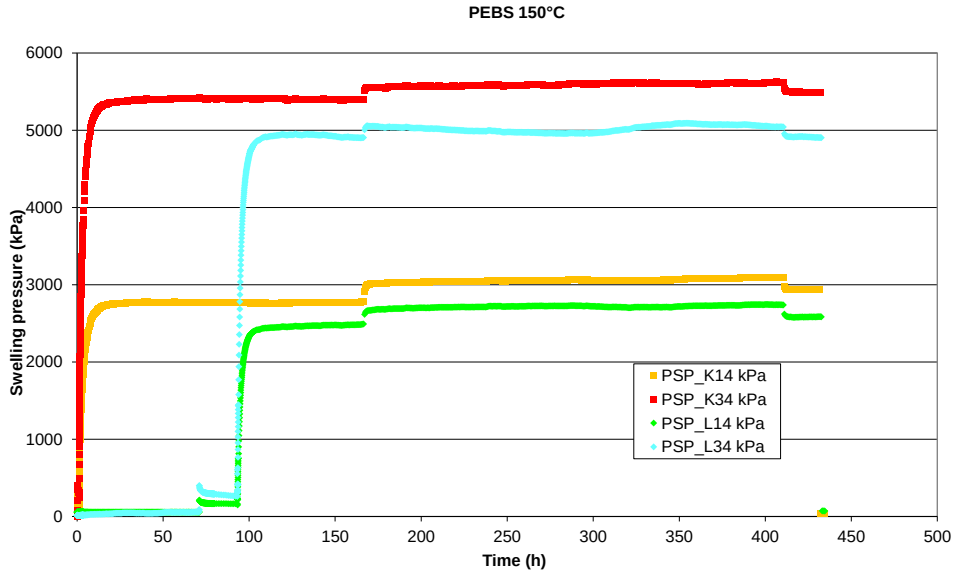

Figure A1-12. Evolution of swelling pressure of specimens exposed to 150°C in series K&L.

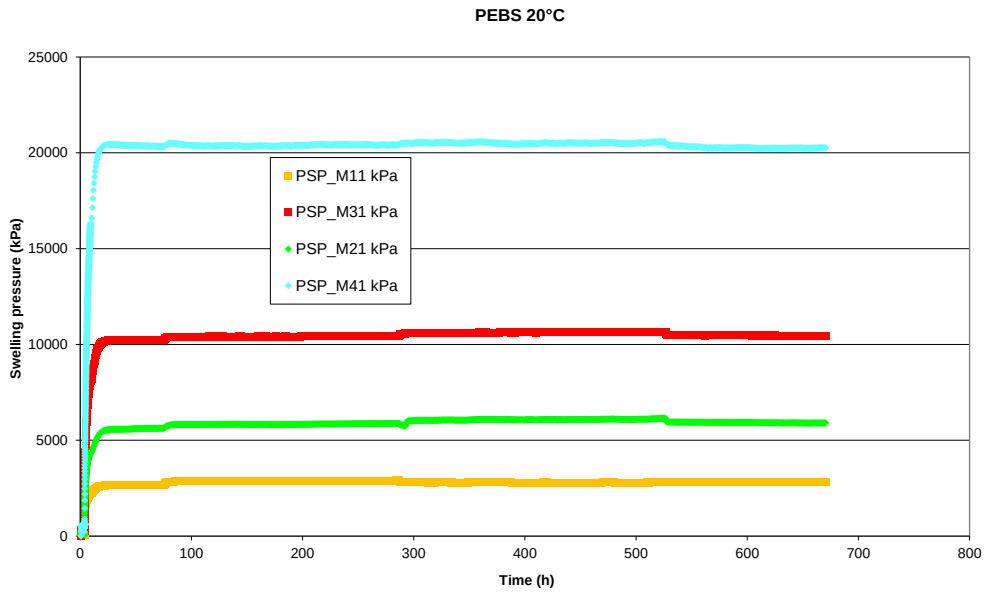

Figure A1-13. Evolution of swelling pressure of reference specimens in M.

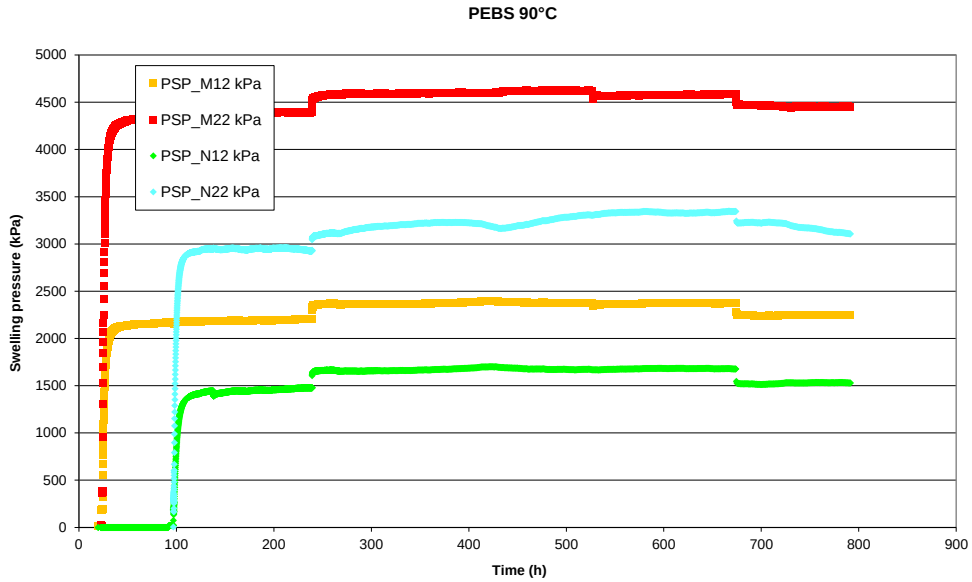

Figure A1-14. Evolution of swelling pressure of specimens exposed to 90°C in series M&N.

A1.2 Tables

A1.2.1 Results from unconfined compression tests

Table A1-1. Test results from PUC tests on mainly MX-80 specimens. For evaluation of S_r ρ_w = 1000 kg/m^3 and ρ_s = 2780 kg/m^3 were used.

Test ID	Material	Final values			At shearing		Max T
		ρ_d	w	S_r	q_{max}	ε	
		kg/m^3	%	%	kPa	%	°C
PUC A1	WyNa	1430	34.3	102	1460	4.1	150
PUC A2	WyNa	1520	30.1	103	2570	2.7	150
PUC A3	MX-80	1520	29.5	99	2390	5.2	150
PUC A4	WyNa	1480	31.8	102	1680	7	20
PUC A5	WyNa	1560	28.5	103	2060	4.8	20
PUC A6	MX-80	1600	26	98	3040	8.2	20
PUC B1	MX-80	1490	30.6	98	1830	9.2	20
PUC B2	MX-80	1570	27.2	98	2610	7.9	20
PUC B3	MX-80G	1480	31.7	100	1720	10.3	20
PUC B4	MX-80G	1480	31.7	100	1730	9	20
PUC B5	MX-80G	1560	27.9	100	2640	8.8	20
PUC B6	MX-80G	1580	27.2	99	2910	8.8	20
PUC B7	MX-80G fine	1460	32.5	99	2020	6.3	20
PUC B8	MX-80G fine	1470	31.3	98	2010	5.1	20
PUC B9	MX-80G fine	1560	27.6	98	2880	3.7	20
PUC B10	MX-80G	1600	26.2	98	3320	8.2	20
PUC C1	MX-80	1510	29	96	1810	8.7	20
PUC C2	MX-80	1590	25.9	96	2700	8.3	20
PUC C3	MX-80	1660	23.3	95	3810	6.7	20
PUC C4	MX-80	1490	31	99	1820	9.9	20
PUC C5	MX-80	1590	26.3	97	2960	7.9	20
PUC C6	MX-80	1670	22.9	96	4860	6.2	20
PUC D1	MX-80	1520	29.1	98	2550	7.8	20
PUC D2	MX-80	1490	30.8	99	2180	7.7	20
PUC D3	MX-80 fr	1490	30.8	99	1180	1.6	20
PUC D4	MX-80 fr	1490	30.6	98	1050	1.7	20
PUC D5	MX-80 fr	1480	31.9	101	1040	2.2	20
PUC D6	MX-80	1570	27.2	98	2970	7.3	20
PUC D7	MX-80 fr	1540	28.9	100	1580	1.9	20
PUC D8	MX-80 fr	1550	28.4	100	1640	1.9	20
PUC D9	MX-80 fr	1550	28.4	99	1550	2	20
PUC D10	MX-80 fr	1570	27.5	99	1890	2.2	20

Test ID	Material	Final values			At shearing		Max T
		ρ_d	w	S_r	q_{max}	ε	
		kg/m^3	%	%	kPa	%	°C
PUC E1	MX-80 Na	1480	31.6	99	1190	9.7	20
PUC E2	MX-80 Na	1570	27.4	99	2220	7.7	20
PUC E3	MX-80 Na	1640	24.8	99	3630	7.9	20
PUC E4	MX-80 Ca	1450	33.2	100	1540	8.3	20
PUC E5	MX-80 Ca	1550	28.3	99	2550	7.7	20
PUC E6	MX-80 Ca	1640	24.7	98	3910	6.9	20
PUC F1	MX-80	1470	31.9	99	1660	9.1	20
PUC F2	MX-80	1510	29.7	98	2130	9.1	20
PUC F3	MX-80	1520	29.6	99	2090	8.1	20
PUC F4	MX-80	1570	26.9	97	2750	7.9	20
PUC F5	MX-80wash	1480	31.4	99	2150	5.7	20
PUC F6	MX-80wash	1520	29.6	100	2000	9.1	20
PUC F7	MX-80wash	1580	27.1	100	2880	7	20
PUC F8	MX-80<2	1450	33	100	2040	6.9	20
PUC F9	MX-80<2	1510	29.9	100	2560	5.6	20
PUC F10	MX-80<2	1570	27.5	99	3570	5.1	20
PUC G1	MX-80 +2%CaSO4	1580	26.3	96	1800	5.3	150
PUC G2	MX-80 +2%CaSO4	1590	26.5	98	2890	7.3	20
PUC H1	MX-80axial	1550	28.8	100	2090	9.7	20
PUC H2	MX-80axial	1600	26.2	99	2680	9.2	20
PUC H3	MX-80axial	1550	27.7	98	2170	8.6	20
PUC H4	MX-80radial	1560	27.8	99	2290	9.4	20
PUC H5	MX-80radial	1620	25.2	98	3390	8.6	20
PUC H6	MX-80radial	1560	28	99	2470	9.4	20
PUC I1	MX-80	1570	27.2	98	2770	7.3	20
PUC I2	MX-80	1570	27.4	99	2720	7.9	20
PUC I3	MX-80	1550	27.4	97	2620	8.2	20
PUC I4	MX-80	1570	26.9	97	2790	8.7	20
PUC I5	MX-80	1570	27.9	100	2660	8.2	20
PUC I6	MX-80	1560	27.9	99	2600	8	20
PUC I7	MX-80	1570	27.3	99	2720	8	20
PUC I8	MX-80	1570	27	98	2820	7.9	20
PUC I9	MX-80	1570	27.4	99	2770	8.1	20
PUC I10	MX-80	1570	26.9	97	2800	7.7	20
PUC K12	MX-80	1460	32.2	100	1550	8.9	90
PUC K22	MX-80	1580	27	98	2650	7.9	90

Test ID	Material	Final values			At shearing		Max T
		ρ_d	w	S_r	q_{max}	ε	
		kg/m^3	%	%	kPa	%	°C
PUC K32	MX-80	1650	23.9	96	3890	6	90
PUC L12	MX-80	1460	32.3	99	1750	9.5	90
PUC L22	MX-80	1550	27.9	99	2710	8.5	90
PUC L32	MX-80	1590	26.4	97	3080	9	90
PUC K22c1	MX-80	1570	27.4	99	2840	7.6	90
PUC K22c2	MX-80	1570	27.3	99	2840	8.1	90
PUC K22c3	MX-80	1550	28.2	99	2280	8.2	90
PUC K22c4	MX-80	1570	27.1	98	2020	7.7	90
PUC K22c5	MX-80	1580	27.1	99	2810	7.4	90
PUC K22c6	MX-80	1580	26.6	98	3090	7.1	90
PUC K13	MX-80	1480	31.4	99	1600	9.1	120
PUC K23	MX-80	1550	27.7	97	2420	7.5	120
PUC K33	MX-80	1620	25	96	3170	7.6	120
PUC L13	MX-80	1460	32.2	99	1870	8.5	120
PUC L23	MX-80	1570	27.6	99	3090	7	120
PUC L33	MX-80	1630	24.9	98	4200	5.9	120
PUC K14	MX-80	1480	30.1	96	2050	6.4	150
PUC K24	MX-80	1590	26	96	3470	5.4	150
PUC K34	MX-80	1630	23.6	94	3830	5.6	150
PUC L14	MX-80	1480	32.1	101	2070	6.4	150
PUC L24	MX-80	1570	27.6	99	3160	5.5	150
PUC L34	MX-80	1640	24.9	99	4250	4.7	150

Table A1-2. Test results from PUC tests on FEBEX specimens. For evaluation of S_r ρ_w = 1000 kg/m^3 and ρ_s = 2735 kg/m^3 were used.

Test ID	Material	Final values			At shearing		Max T
		ρ_d	w	S_r	q_{max}	ε	
		kg/m^3	%	%	kPa	%	°C
PUC M11	FEBEX	1390	33.4	95	1110	6.3	20
PUC M11b	FEBEX	1400	33.8	96	1170	7.3	20
PUC M11c	FEBEX	1400*	33		1080	6.6	20
PUC M51	FEBEX	1420	31.4	92	1590	7.5	20
PUC M51b	FEBEX	1460	30.3	95	1530	7	20
PUC M21	FEBEX	1520	27.9	95	2150	6.5	20
PUC M21b	FEBEX	1500	28.9	97	2230	6.7	20
PUC M21c	FEBEX	1510*	28.9		2220	6.3	20
PUC M31	FEBEX	1590	25.7	97	3550	6.5	20
PUC M41	FEBEX	1600	25.4	98	3680	6.6	20
PUC M12	FEBEX	1470	30.3	96	1590	5.8	90
PUC M52	FEBEX	1520	28.2	97	2180	7.2	90
PUC M22	FEBEX	1520	28.1	96	2270	7.1	90

Test ID	Material	Final values			At shearing		Max T
		ρ_d	w	S_r	q_{max}	ε	
		kg/m^3	%	%	kPa	%	°C
PUC N12	FEBEX	1430	32.4	98	1420	5.8	90
PUC N52	FEBEX	1470	29.4	94	2010	7.2	90
PUC N22	FEBEX	1520	28.5	97	2330	7.6	90

** Estimated value*

A1.2.2 Results from swelling pressure and hydraulic conductivity tests

Table A1-3. Test results from PSP tests on MX-80 specimens. For evaluation of S_r ρ_w = 1000 kg/m^3 and ρ_s = 2780 kg/m^3 were used.

Test ID	Material	Final values			Swelling pressure		Hydraulic conductivity			Max T
		ρ_d	w	S_r	$P_{s,start}$	$P_{s,final}$	gradient	k_w	$k_{w,corr}$	
		kg/m^3	%	%	kPa		m/m	m/s		°C
PSP K11	MX-80	1400	35.3	99	2460	2610	3900	1.9E-13	2.0E-13	20
PSP K11b	MX-80	1550	28.8	100	6600	6740	10600	6.7E-14	7.0E-14	20
PSP K21	MX-80	1590	27.2	100	7770	8080	9900	8.7E-14	9.1E-14	20
PSP K31	MX-80	1600	26.5	99	9450	9540	9500	5.5E-14	5.9E-14	20
PSP K12	MX-80	1400	34.5	98	2460	2600	5000	2.1E-13	2.2E-13	90
PSP K32	MX-80	1530	29.6	101	4810	5030	4900	2.1E-13	9.6E-14	90
PSP L12	MX-80	1380	36.6	100	2320	2460	4900	1.3E-13	1.4E-13	90
PSP L32	MX-80	1500	30.5	99	5140	5250	4900	6.7E-14	7.7E-14	90
PSP K13	MX-80	1410	34.5	99	2570	2780	5000	1.3E-13	1.6E-13	120
PSP K33	MX-80	1550	27.9	98	5400	5670	5100	6.6E-14	8.3E-14	120
PSP L13	MX-80	1410	35.2	100	2740	2840	5100	1.3E-13	1.5E-13	120
PSP L13	MX-80	1530	29.1	99	5490	5650	4800	6.9E-14	8.3E-14	120
PSP K14	MX-80	1410	34.9	100	2770	2620	5100	1.6E-13	1.7E-13	150
PSP K34	MX-80	1540	28.6	99	5400	5490	4600	7.0E-14	7.4E-14	150
PSP L14	MX-80	1380	36.1	99	2480	2300	5000	1.2E-13	1.4E-13	150
PSP L14	MX-80	1520	29.7	100	4900	4910	4600	5.6E-14	7.7E-14	150

Table A1-4. Test results from PSP tests on FEBEX specimens. For evaluation of S_r ρ_w = 1000 kg/m^3 and ρ_s = 2735 kg/m^3 were used.

Test ID	Material	Final values			Swelling pressure		Hydraulic conductivity			Max T
		ρ_d	w	S_r	$P_{s,start}$	$P_{s,final}$	gradient	k_w	$k_{w,corr}$	
		kg/m^3	%	%	kPa	kPa	m/m	m/s	m/s	°C
PSP M11	FEBEX	1420	33.8	99	2690	2800	4900	2.6E-13	PSP M11	20
PSP M21	FEBEX	1500	29.3	97	5620	5900	9800	8.0E-14	PSP M21	20
PSP M31	FEBEX	1580	25.7	96	10240	10460	9400	4.4E-14	PSP M31	20
PSP M41	FEBEX	1650	22.9	95	20350	20250	10000	3.5E-14	PSP M41	20

Test ID	Material	Final values			Swelling pressure		Hydraulic conductivity			Max T
		ρ_d	w	S_r	$P_{s,start}$	$P_{s,final}$	gradient	k_w	$k_{w,corr}$	
		kg/m^3	%	%	kPa	kPa	m/m	m/s	m/s	°C
PSP M12	FEBEX	1400	35.0	100	2210	2250	4800	1.6E-13	1.8E-13	90
PSP M22	FEBEX	1480	30.6	99	4390	4460	4600	8.1E-14	9.8E-14	90
PSP N12	FEBEX	1370	36.8	102	1480	1530	4900	2.3E-13	2.5E-13	90
PSP N22	FEBEX	1440	33.0	100	2930	3120	4900	1.0E-13	1.2E-13	90

A2 Analysis of influence of temperature, deviations from best fit lines

Best fit lines for the reference tests regarding the maximum deviator stress at failure $q_{max,bf}$, the corresponding strain ε_{bf}, the swelling pressure $P_{s,bf}$ and the hydraulic conductivity $k_{w,bf}$ were determined, Equations A-1 to A-4 and Table A2-1 and Table A2-2. For each parameter the relative differences between the measured values from the reference specimens and the corresponding best fit line were calculated according to Equation A-5. For each parameter the standard deviation of these relative differences was calculated and given in the tables below.

$$q_{max,bf} = A \cdot e^{B \cdot \rho_d} \quad \text{(A-1)}$$

$$\varepsilon_{bf} = C \cdot \rho_d + D \quad \text{(A-2)}$$

$$P_{s,bf} = K \cdot e^{L \cdot \rho_d} \quad \text{(A-3)}$$

$$k_{w,bf} = M \cdot {\rho_d}^N \quad \text{(A-4)}$$

$$rel.dif. = \frac{measured\ value\ - best\ fit\ line(\rho_d)}{best\ fit\ line\ (\rho_d)} \quad \text{(A-5)}$$

Table A2-1. Constants (A, B) and (C, D) corresponding to the best fit lines for the reference tests on maximum deviator stress at failure $q_{max,bf}$ (Equation 1) and corresponding strain ε_{bf} (Equation 2), respectively. The standard deviations (std. dev.) of the relative differences are also given as well as the valid dry density intervals.

Material	Deviator stress $q_{max,bf}$			Strain at failure ε			No of test	Dry density interval	
	A	B	std. dev	C	D	std.dev.		Min kg/m³	Max kg/m³
MX-80	1.53	0.0048	0.05	-0.011	24.6	0.06	26	1450	1670
FEBEX	0.45	0.0056	0.08	-0.0021	9.9	0.05	10	1390	1600

Table A2-2. Constants (K, L) and (M, N) corresponding to the best fit lines for the reference tests on swelling pressure $P_{s,bf}$ (Equation 3) and hydraulic conductivity $k_{w,bf}$ (Equation 4), respectively. Valid dry density intervals are also mentioned. The standard deviations (std. dev.) of the relative differences are also given as well as the valid dry density intervals.

Material	Swelling pressure P_s			Hydraulic conductivity k_w			No of tests	Dry density interval	
	K	L	std. dev.	M	N	std. dev.		Min kg/m³	Max kg/m³
MX-80	0.41	0.0063	0.035	3.6E+12	-8.0	0.19	4	1400	1600
FEBEX	0.024	0.008	0.033	7.6E+29	-13.5	0.21	4	1420	1650

Specimens of MX-80 were exposed to 90°C, 120°C and 150°C and specimens of FEBEX were exposed to 90°C during 24h. Heating was made after or before full saturation where heating after full saturation was done with a controlled water pressure while heating before full saturation meant heating at a high degree of saturation without control of the water pressure but under sealed conditions.

The relative differences, according to Equation A-5, were also calculated for the test results from the heated specimens and these values are compared with corresponding values of the reference specimens in Figures A2-1 to A2-6. The diagrams and tables are given as a complement to the analysis in Chapter 5.

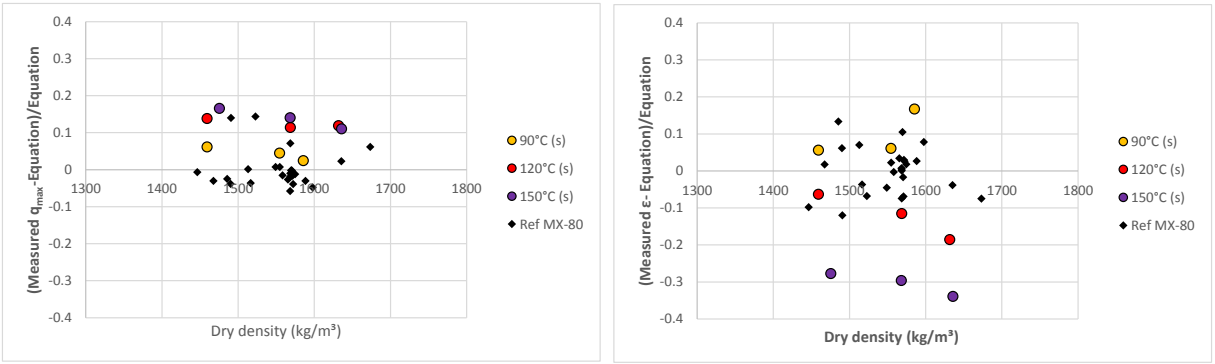

Figure A2-1. The relative differences (Equation A-5) calculated for maximum deviator stress at failure and corresponding strain for MX-80 specimens exposed to heating under saturated conditions.

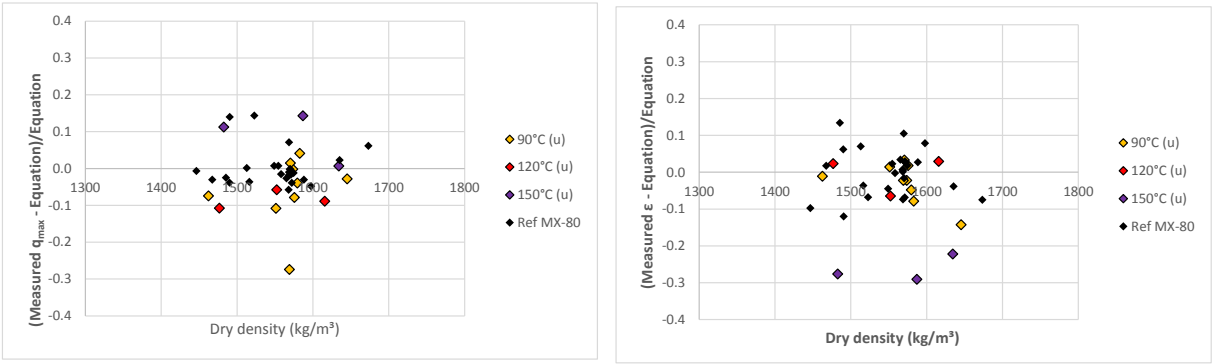

Figure A2-2. The relative differences (Equation A-5) calculated for maximum deviator stress at failure and corresponding strain for MX-80 specimens exposed to heating under conditions with no compensating water pressure.

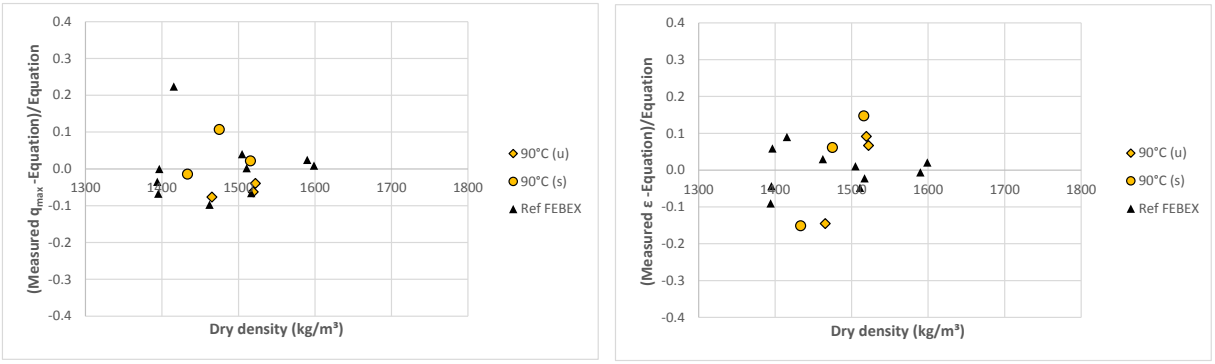

Figure A2-3. The relative differences (Equation A-5) calculated for maximum deviator stress at failure and corresponding strain for all FEBEX specimens exposed to 90°C.

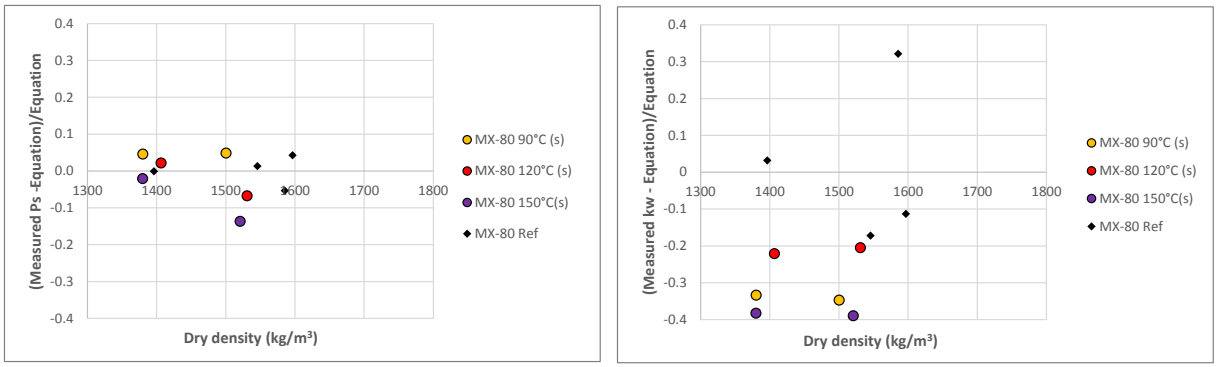

Figure A2-4. The relative differences (Equation A-5) calculated for swelling pressure and hydraulic conductivity for MX-80 specimens exposed to heating under saturated conditions.

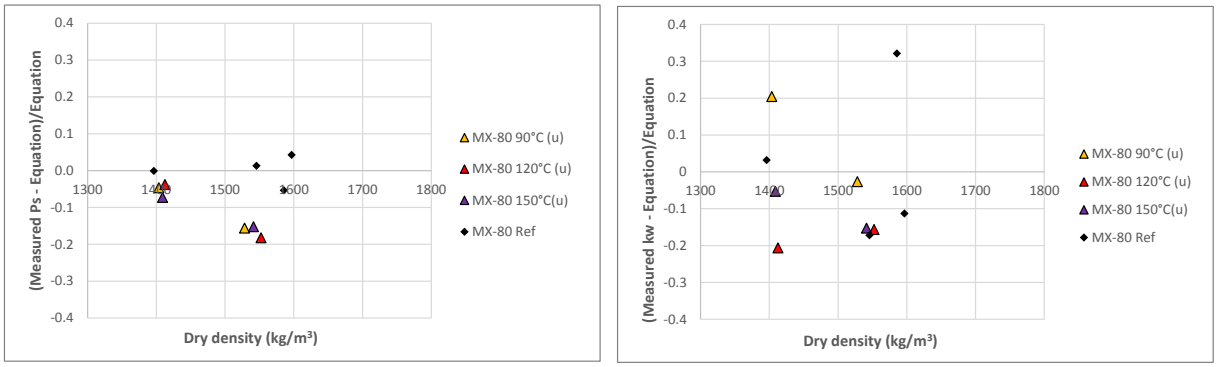

Figure A2-5. The relative differences (Equation A-5) calculated for swelling pressure and hydraulic conductivity for MX-80 specimens exposed to heating under conditions with no compensating water pressure.

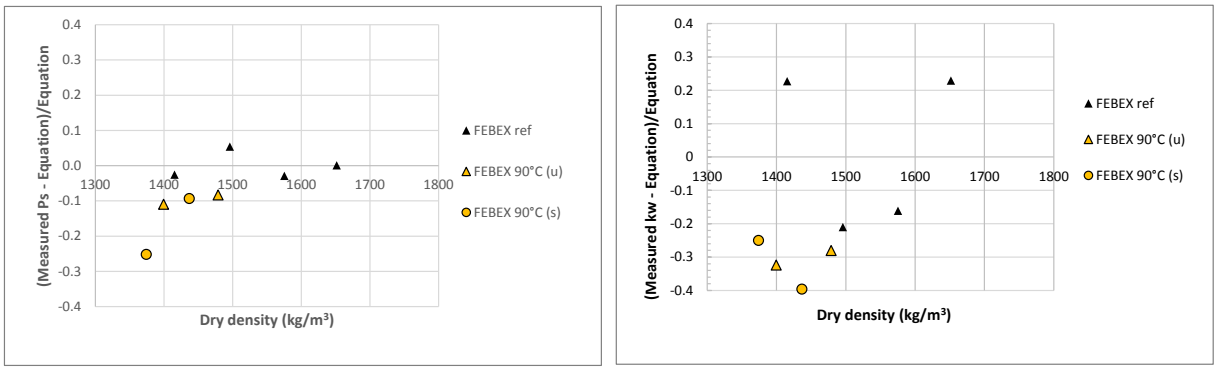

Figure A2-6. The relative differences (Equation A-5) calculated for swelling pressure and hydraulic conductivity for all FEBEX specimens exposed to 90°C.

A3 Test series; number of specimens and time used

Table A3-1. Test series of unconfined compression tests with the main objectives of each series, the material used, the maximum temperatures used during the short-term heating, the number of specimens in each series and the total time used.

Series	Main objective	Material	Water other than de-ionized	T_{max} during 24h of exposure	Number of specimens	Total number of days, approx.
A	Influence of heat on purified Na bentonite	WyNa		150°	2+2	25
B	Influence of grinding and separation of coarse fra	MX-80		20°	10	24
C	Influence of saturation with CaCl2	MX-80	0.3MCaCl2	20°	6	40
D	Influence of introduced fractures	MX-80		20°	10	45+63
E	Influence of circulation with Na2SO4	MX-80	1M Na2SO4	20°	6	147
F	Influence of washing	MX-80		20°	10	42
G	Influence of content of CaSO4	MX-80+CaSO4		150°	1+1	75+378
H	Influence of direction of compaction	MX-80		20°	6	14
I	Check of variability	MX-80		20°	10	17
K	Influence of heating before/after saturation	MX-80		90°	6	46
K,L	Influence of heating before/after saturation	MX-80		90°	3+3	33 / 13+19
K,L	Influence of heating before/after saturation	MX-80		120°	3+3	20 / 10+11
K,L	Influence of heating before/after saturation	MX-80		150°	3+3	19 / 14+5
M	Reference specimens	FEBEX		20°	10	57
M,N	Influence of heating before/after saturation	FEBEX		90°	3+3	21 / 10+13

Table A3-2. Test series of swelling pressure and hydraulic conductivity test with the main objectives of each series, the material used, the maximum temperatures used during the short-term heating, the number of specimens in each series and the total time used.

Series	Main objective	Material	Water other than de-ionize	T_{max} during 24h of exposure	Number of specimens	Total number of days, approx.
K,L	Influence of heating before/after saturation	MX-80		20°	4	28
K,L	Influence of heating before/after saturation	MX-80		90°	2+2	115 / 13 + 101
K,L	Influence of heating before/after saturation	MX-80		120°	2+2	56 / 10+47
K,L	Influence of heating before/after saturation	MX-80		150°	2+2	40 / 14 + 25
M	Reference specimens	FEBEX		20°	4	28
M,N	Influence of heating before/after saturation	FEBEX		90°	2+2	55 / 10 + 46